An *in-vivo* analysis of SLMAP function in the postnatal mouse myocardium

By:

Taha Rehmani

A thesis submitted to the Faculty of Graduate and Postdoctoral Studies in partial fulfillment of the requirements of the M.Sc. degree in Cellular and Molecular Medicine

Department of Cellular and Molecular Medicine

Faculty of Medicine

University of Ottawa,

Ottawa, Ontario, Canada

Abstract:

SLMAP is a tail anchored membrane protein that alternatively splices to generate three isoforms, SLMAP1, SLMAP2 and SLMAP3. Previous studies in our lab have shown that the postnatal cardiac-specific overexpression of SLMAP1 results in intracellular vesicle expansion and enhanced endosomal recycling. I generated a postnatal cardiac-specific knockout model using the Cre-Lox system to nullify all three SLMAP isoforms and further evaluate its role in the mouse myocardium. SLMAP knockdown and knockout mouse hearts were analyzed with western blotting and qPCR. I found that only SLMAP3 was nullified and phenotypic evaluation through echocardiography indicated that young and old SLMAP3 knockout animals showed no remarkable changes in cardiac function. Furthermore, challenge with stressor isoproterenol had a similar response to wildtype and knockout mice in cardiac structure and function. Surprisingly the level of expression of SLMAP1 and SLMAP2 was maintained in the myocardium from SLMAP3 deficient mice. Interestingly the machinery involved in endosomal recycling was not impacted by the loss of SLMAP3. These data indicate that loss of SLMAP3 does not alter cardiac structure and function in the postnatal myocardium in the presence of SLMAP1 and SLMAP2.

Table of Contents

LIST OF FIGURES:

LIST OF TABLES:

LIST OF ABBREVIATIONS

α-MyHC	alpha myosin heavy chain
αSNAP	Alpha soluble N-ethylmaleimide-sensitive factor attachment protein
ANOVA	Analysis of variance
ATP	Adenosine triphosphate
β-MyHC	Beta myosin heavy chain
CDE	Clathrin dependent endocytosis
CFTR	Cystic fibrosis transmembrane conductance regulator
CIE	Clathrin independent endocytosis
Cre	Causes recombination
DCM	Dilated cardiomyopathy
EC	Excitation-contraction
ECHO	Echocardiography
ECM	Extracellular matrix
EEA1	Early endosomal antigen 1
EF	Ejection fraction
ER	Endoplasmic reticulum
ERC	Endosomal recycling complex
EsR	Estrogen receptor
FACS	Fluorescent-activated cell sorting
FHA	Forkhead associated domain
Flox	Flanked with loxP
FS	Fractional shortening
GLUT4	Glucose transporter 4
GSV	GLUT4 storage vesicle
H&E	Hematoxylin and Eosin
HBD	Hormone binding domain
HCM	Hypertrophic cardiomyopathy
Hs90	Heat shock 90 protein
I.P.	Intraperitoneal
ISO	Isoproterenol
IVS; s/d	Intraventricular septum; diastole/systole

KD	Knockdown
KO	Knockout
LV	Left Ventricle
LVID; s/d	Left ventricular intradiameter; diastole/systole
LVPW; s/d	Left ventricular posterior wall; diastole/systole
MER	Modified estrogen receptor
MTOC	Microtubule organizing center
NSF	N-ethylaleimide-sensitive factor
PCR	Polymerase chain reaction
PEST	Proline Argnine Serine Threonine riched domain
RBPTN-5	Rabaptin-5
SDS-PAGE	Sodium dodecyl sulfate polyacrylamide gel electrophoresis
sgRNA	Single guide RNA
siRNA	Small interfering RNA
SLMAP	Sarcolemmal membrane associated protein
SNAP	Synaptosomal-associated proteins
SNARE	Soluble N-ethylamide-sensitive factor activating protein receptors
SR	Sarcoplasmic reticulum
TBST	Tris-buffered saline tween
TG	Transgenic
TGN	Transgolgi network
TM1/TM2	Transmembrane domain 1/2
VAMP	Vesicle associated membrane protein
Wt	Wildtype

ACKNOWLEDGEMENTS

First and foremost, I'd like to thank Dr. Balwant Tuana for his fantastic mentorship that helped me achieve my first graduate degree. By constantly motivating and pushing me it resulted in allowing me to achieve a higher plane of learning. His support during the lows and his banter during the highs provided a unique balance that was essential in keeping myself content and grounded during my master's tenure.

I would also like to thank the members of the Tuana Lab. My first thanks goes out to Maysoon Salih, whose experience and advice ensured the best results for my experiments. Secondly, I would like to thank Jenn and Jana for patiently training me, providing creative input, being an extra set of eyes for analysis and ears for frustration. A special mention also goes out to Aaraf.

I would like to thank my family. My parents, Nadeem and Uzma, for providing me with intellectual dialogue, self-confidence, and a full belly thus allowing me to mature to become the person I am today. My first-generation siblings, Unaiz and Umar, for being live-in friends that provided laughter, non-judgemental late night snacking and nighttime mischief. My second-generation siblings, Ayesha and Humza, for being the apples of my eye and choosing me to be the template of their individual success.

Finally, I'd like to thank Arsenal FC. We've had some lows, we've had some highs, but there's no other club I'd rather support.

Chapter 1: Introduction

1.1 The mammalian heart structure and function

The heart is the main component of the cardiovascular system, it is an organ composed of four-chambers that collects and distributes blood (Hall, 2011). The four chambers of the mammalian heart consist of the right atrium, right ventricle, left atrium and left ventricle (Standring & Borley, 2008). The heart is mostly made up of cardiac muscle (myocardium) and composed of heart-specific muscle cells known as cardiomyocytes (Heusch & Schulz, 1996). A heartbeat is regulated by systole and diastole named for the synchronous contraction and relaxation of the myocardium (Hall, 2011). The right heart mediates pulmonary circulation while the left heart mediates systematic circulation. Pulmonary circulation begins with the accumulation of deoxygenated blood in the right atrium during diastole after which it enters the right ventricle which contracts to push blood to the lungs via the pulmonary artery during systole (Standring & Borley, 2008). During diastole and systole in systemic circulation, the left atrium collects oxygenated blood from the lungs, allows it to enter the left ventricle which then contracts to diffuse the newly oxygenated blood to the entire body via the aorta (Fukuta & Little, 2008). Systemic circulation results in the left ventricle (LV) being significantly larger than the other chambers due to the diversity of blood delivery through this ventricle (Standring & Borley, 2008). Systole and diastole are regulated via electrical conductions and ATP energy transfer that work in tandem to facilitate myocardium contraction (Severs, 2000).

Heart disease is the second leading cause of death in Canada (Statistics Canada, 2014). A specific type of heart disease, cardiomyopathy, is a disease which leads to structural changes within the myocardium (Yacoub, 2014). The two common phenotypic classifications of cardiomyopathies are hypertrophic cardiomyopathy (HCM) and dilated cardiomyopathy (DCM) (Wexler, et al., 2009). These cardiomyopathies are defined to take place 'in the absence of coronary heart disease, hypertension, valvular or congenital heart disease' (Yacoub, 2014). These structural changes are a result of pathological cardiac remodeling, which occurs when the heart attempts to compensate for a pressure or volume overload by enlarging the LV (Burchfield, et al., 2013).

HCM is characterized by asymmetric hypertrophy, resulting in a significant thickness of the LV myocardium (Hensley, et al., 2015). This pathological hypertrophy results in decreased cardiac function and is identified as an early symptom of heart failure (Marian & Roberts, 2001). HCM is a genetic disease with autosomal dominant inheritance thus HCM patients usually have a family history of cardiomyopathy (Hensley, et al., 2015). Research spanning the last decade has identified over 100 mutations spanning ten genes which result in HCM (Wexler, et al., 2009). It is estimated that 35-50% of HCM cases are caused by a mutation in a single gene, β-myosin heavy chain (β-MyHC) which has over 60 identified mutations which directly result in HCM (Marian & Roberts, 2001; Seidman & Seidman, 1998). Other genes that cause HCM are also cardiac contractile proteins such as cardiac troponin and myosin-binding protein C (Carrier, et al., 1997; Seidman & Seidman, 1998).

DCM is the most common characterized cardiomyopathy that also enlarges the LV but through a different mechanism. Patients exhibiting DCM have thin and stretched LV walls, that result in reduced systolic function (Luk, et al., 2009). Thinning of the myocardium also causes cardiomyocyte necrosis, triggering disorganization of the contractile function within cardiomyocytes (Westendorp, et al., 2012). DCM is also caused by genetic mutations in cardiac contractile protein units such as myosin heavy chain and troponin (McNally, et al., 2013) . Most recently, it has been discovered to be linked to a mutation in titin (Herman, et al., 2012). Titin is the largest human protein, involved in sarcomere assembly and aids in contraction of the skeletal muscle and myocardium (Tskhovrebova & Trinick, 2003). Research on titin over the past decade has uncovered 72 unique mutations present within the gene resulting in DCM (Herman, et al., 2012). Overall titin was responsible for approximately 25% of DCM in humans (Herman, et al., 2012). Interestingly, both cardiomyopathies are a result of mutated proteins localized to the sarcomere driving the implication that alterations to cardiac structure can result in changes to cardiac function.

1.2 Cardiomyocytes regulate myocardial function

Cardiomyocytes are the main regulators of myocardium contraction and relaxation by mediating action potentials and metabolizing energy (Severs, 2000). Each individual cardiomyocyte is highly organized, dynamic and always active. Cardiomyocytes are non-proliferative and non-regenerating, as cardiomyocytes exit the cell cycle a few days after birth (Mahmoud, et al., 2014). Carbon dating

experiments revealed that between the ages 25-75, cardiomyocyte turnover decreases from 1% to 0.45% (Bergmann, et al., 2009). Cardiomyocyte undergo a significant amount of physical stress due to beating continuously, therefore their regulation is essential especially when considering the low turnover rate.

The cardiomyocytes contain the functional unit of contraction, the sarcomere. The sarcomere consists of Z lines, thin, thick and elastic filaments (Xiao & Shaw, 2015). The sarcomere of cardiomyocytes is highly integrated into the excitation-contraction (EC) coupling which include three crucial structural entities: the t-tubule domain, intercalated disc at the cell-cell junction, and the lateral membrane domain (Balse, et al., 2012). The t-tubule domains are invaginations of the plasma membrane (sarcolemma) that interact with the sarcoplasmic reticulum (SR) and through this interaction mediate calcium ion homeostasis in the cardiomyocyte (Ibrahim, et al., 2011). The intercalated discs are involved in cell-cell interaction between cardiomyocytes, mostly through fascia adherens, desmosomes and gap junctions (Kleber & Saffitz, 2014). Finally, the lateral membrane will bind to the extracellular matrix (ECM) to aid cardiomyocyte contraction within a three-dimensional space (Balse, et al., 2012).

The contraction of cardiomyocytes are generated through cardiac action potentials which are carried forward by plasma membrane ions channels that accurately control calcium (Ca^{2+}), sodium (Na^{+}), and potassium (K^{+}) ions (Nerbonne & Kass, 2005). During systole, the initial inward flux of Na^{+} ions through sodium channels causes depolarization on the membrane (Santana, et al., 2010). This influx activates the voltage gated Ca^{2+} exchanger present on the t-

tubule to interact with the SR calcium exchanger to push Ca^{2+} from the SR to the cytosol (Amin, et al., 2010). This free Ca^{2+} will generate a contraction through interaction with troponin C and the thick and thin filaments (Yin, et al., 2015). Finally, the outward flux of K^{+} ions repolarizes resetting the heart back to diastole (Woodcock & Matkovich, 2005). Many disease models are associated with ion channels. The disease models range from trafficking defects to genetic mutations mainly resulting in different types of cardiac arrhythmias (irregular heartbeat). Several irregular ion channels cause a long QT syndrome, resulting in ventricular tachycardia and ventricular fibrillation (Amin, et al., 2010). Timothy syndrome, a multisystem disease causing QT interval prolongation, ventricular tachyarrhythmia, and structural heart disease was linked to mutations in Ca^{2+} ion channel, $Ca_v1.2$ (Bett, et al., 2012).

There is a tremendous need for energy (ATP) in the cardiomyocyte during both systole and diastole. Thus the mitochondria, where cellular respiration occurs, are highly abundant within the cardiomyocyte and compose ~35% of the cell volume (Pasqualini, et al., 2016). Metabolic processes can be altered based on age and overall health of the individual's heart. In the fetal heart, energy consumption consists mainly of ATP production via glycolytic pathways, while mature hearts derive energy from fatty acid oxidation (Pasqualini, et al., 2016). In a compromised heart, there are alterations in substrate utilization as well as increased demand for ATP. In the failing adult heart, glycolytic pathways increase to aid in the production of ATP due to dead muscle unable to contribute (Gimeno, et al., 2003). However, in a diabetic heart, fatty acid oxidation is significantly

higher, which leads to a significant amount of oxidative stress which hinders the normal function of the heart resulting in diabetic cardiomyopathy (How, et al., 2006).

The common symptom of type 2 diabetes is the decrease transport of glucose through the cell membrane, including cardiomyocytes which puts affected patients at a great risk for diabetic cardiomyopathy (Boudina & Abel, 2010). Evidence has shown that the mechanism through which glucose transport is hindered is predominantly linked to the insulin-dependent glucose transport protein, GLUT4. GLUT4 is a transmembrane protein that localizes to the plasma membrane after insulin-signalling, however in type 2 diabetes insulin sensitivity is decreased thus resulting in the decreased trafficking of GLUT4 to the plasma membrane (Brewer, et al., 2014). Thus, it has been claimed that diabetes and consequently diabetic cardiomyopathy is a result of impaired trafficking of GLUT4 to the plasma membrane. Thus suggesting that the normal expression and regulation of metabolite transport proteins on the cell surface is critical for healthy heart function (Mueckler, 2001).

Cardiomyocyte are dynamic and constantly contracting through electric signals and ATP production. The localization of membrane proteins, metabolite and ion channels are essential and must be highly regulated for the normal function of the cardiomyocyte (Harkcom & Abbott, 2010).

1.3 Intracellular trafficking in the cardiomyocyte

The process of transporting membrane bound proteins to their appropriate domains is known as intracellular trafficking. This is understood by observing the appropriate trafficking mechanisms of membrane proteins, as well as the minute machinery involved in their transport. Primarily, for the regulated expression of membrane proteins, which are essential to transport large metabolites into the cell to metabolize for energy and for the expression of ion channels to regulate ion (Ca^{2+}, Na^{+}, K^{+}) homeostasis within the cardiomyocyte.

Intracellular trafficking can be grouped into two categories: exocytosis which is the movement of vesicle-bound proteins towards the plasma membrane for surface expression and endocytosis which is the internalization of these proteins back to vesicles within the cell (Jahn & Südhof, 1999). Vesicle trafficking is mediated by specialized GTPases called Rab proteins. There are approximately 60 Rab variants, which are involved in a different part of vesicle trafficking and fusion (discussed below) (Segev, 2001).

Exocytosis begins at the endoplasmic reticulum (ER), where most of the membrane protein synthesis takes place. The ER shuttles the vesicle-bound proteins via Rab1 towards the trans-golgi network (TGN) and Rab2 prevents retrograde trafficking of pre-Golgi vesicles back to the ER (Brandizzi & Barlowe, 2014). Membrane proteins are packaged into vesicle membranes at the Golgi apparatus and via regulation of various Rab proteins are trafficked towards the plasma membrane or a membrane bound organelle (Brandizzi & Barlowe, 2014). The regulation of the insulin-dependent GLUT4 and its exocytosis trafficking

patterns have been studied extensively. GLUT4 is synthesized in the ER and packaged in specialized vesicles called GLUT4 storage vesicle (GSV) (Brewer, et al., 2014) which can be identified by the presence of Rab8 and/or Rab10 on the vesicle surface. The GSV remains dormant until it is stimulated by insulin after which it will fuse with the plasma membrane (Foley, et al., 2011).

The half-life expression of membrane proteins is remarkably short on the cell surface, spanning several hours, therefore internalization or endocytosis of the protein is essential for its regulation (Xiao & Shaw, 2015). Endocytosis is divided into clathrin-dependant (CDE) or clathrin-independent endocytosis (CIE) (**Figure 1**). Clathrin surrounds membrane proteins that are fated for internalization which accounts for ~40-50% of endocytosis in the cardiomyocyte (Maxfield & McGraw, 2004). Following CDE and the uncoating of clathrin, the vesicle fuses and transfers its cargo to the early endosome via Rab5. Rab5 recruits a tethering protein, Rabaptin-5 which binds early endosomes to one another (Zhu, et al., 2004). It can also recruit early endosome antigen 1 (EEA1) to allow the early endosomes to dock to one another. This allows the SNARE fusion proteins to interact and drive membrane fusion (Grant & Donaldson, 2009). The membrane proteins in these newly matured early endosomes can then either undergo recycling or degradation through fusion with specialized endosomes that are involved in either pathway (Maxfield & McGraw, 2004).

In the recycling pathway, early endosomes can be redirected to the plasma membrane in a slow or rapid mechanism (**Figure 1**). In the rapid mechanism, early endosomes fuse with the plasma membrane through a Rab

GTPase initially determined to be Rab4 (Deneka, et al., 2003). This was contested due to the increase in rapid recycling results noted when a knockdown of Rab4 was accomplished (Yudowski, et al., 2009). Recent studies have shown that Rab35 is more important in rapid recycling since its depletion resulted in the impairment of the recycling of the transferrin receptor (Kouranti, et al., 2006). In slow recycling, the early endosome fuse with Rab11 endosomes which are called recycling endosomes. These recycling endosomes aggregate and fuse with a long organelle known as the endosomal recycling complex (ERC) (Grant & Donaldson, 2009). Recycling endosomes bud off this complex via Rab11 similarly to the TGN and eventually fuse back to the plasma membrane (Ullrich, et al., 2005).

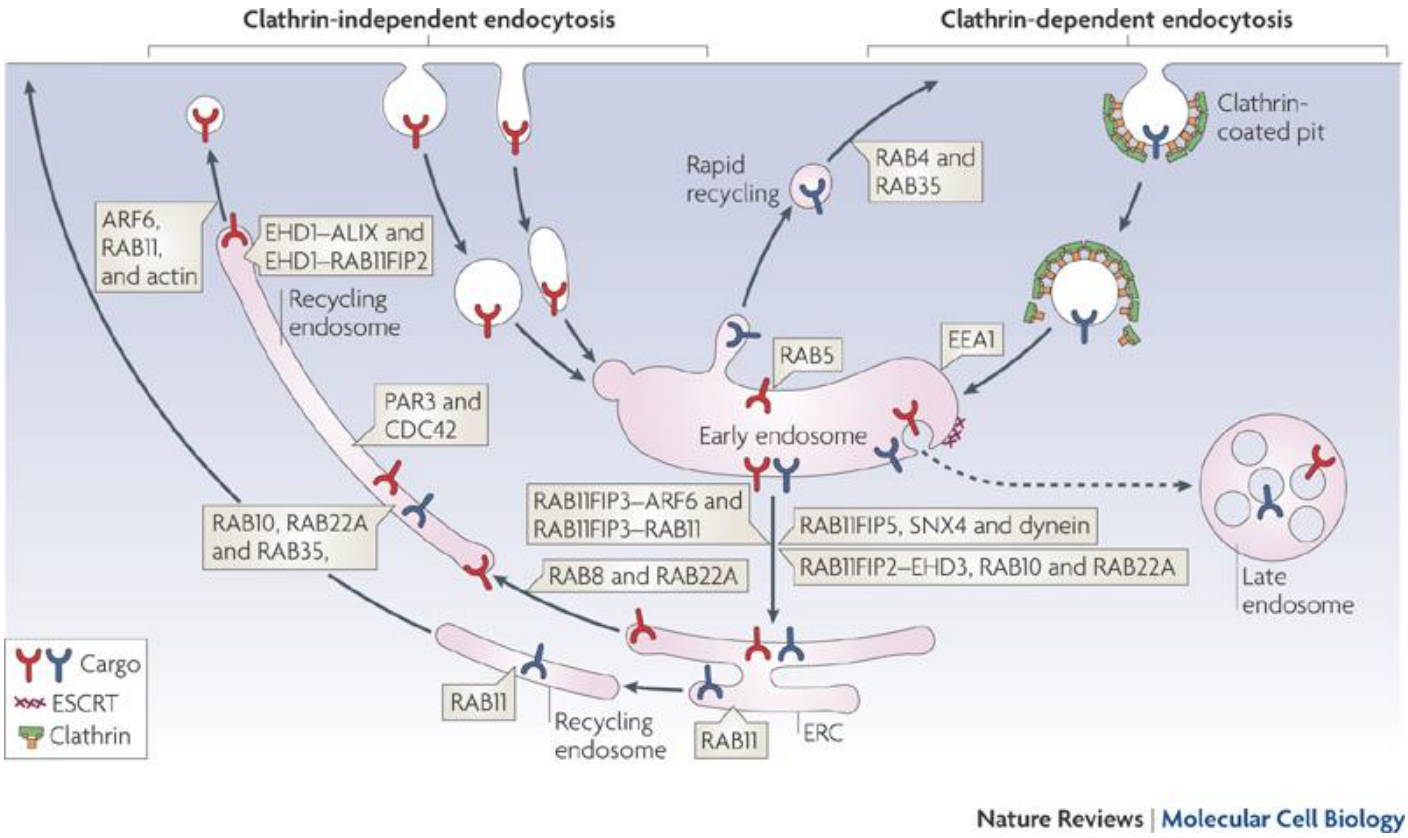

Figure 1. *Overview of endocytic trafficking pathways*. Endocytic trafficking are separated into two groups, clathirin-dependant and clathirin-independent pathways. Both pathways lead to vesicles fusing to form early endosomes which can then direct the cargo towards recycling or degrading. Figure reprinted with permission from (Grant et al, 2009). Copyright (2009) Nature Publishing Group.

As previously mentioned, not all membrane proteins are recycled, a significant portion are shunted towards degradation. Rab7 GTPase endosomes or late endosomes appear to push these proteins towards lysosomes for degradation. The cystic fibrosis transmembrane conductance regulator (CFTR) membrane protein trafficking has been studied extensively since defects in CFTR can result in cystic fibrosis (Skach, 2000). Evidence has shown that overexpression of Rab7 lead to a decrease while expression of a Rab7-dominant negative resulted in an increase in the intracellular pool of CFTR, thereby indicating that Rab7 plays a significant role towards CFTR degradation (Gentzsch, et al., 2004).

Here we can note the significance of Rab GTPases which play crucial roles in the fate of membrane proteins for recycling or degradation. However, the membrane fusion events are not mediated by Rab but by soluble N-ethylamide-sensitive factor activating protein receptor (SNARE) proteins. These SNARE proteins are essential to investigate the machinery involved in trafficking events (Cai, et al., 2007).

1.4 SNARE complexes are essential for membrane fusion to take place

SNARE proteins are a large superfamily of tail anchored membrane proteins which regulate membrane fusion of different vesicles within cells, including the cardiomyocyte (Peters, et al., 2006). All SNARE variants contain a SNARE motif consisting of 60-70 amino acids containing eight heptad repeats. Each SNARE variant can be distinguished structurally as a Q-SNARE or an R-SNARE. The structural differences between these is the single residue glutamine

(Q) or arginine (R) in the SNARE motifs (Hong, 2005). The three families of proteins that contain the SNARE motif are vesicle-associated membrane protein (VAMP), Syntaxin, and Synaptosomal-associated protein (SNAP) (Ramakrishnan, et al., 2012). These proteins alternatively splice to form isoforms that are localized in different organelles, such as the secretory or endocytic pathways (Söllner, et al., 1993). Table 1 highlights the different SNARE protein isoforms and their subcellular localization. VAMPs are structurally identified as R-SNAREs but are simply referred to as v-SNAREs as they are mostly present on the vesicle membrane (Hu, et al., 2003). Syntaxin and SNAPs are structurally identified as Q-SNARE and are referred to as t-SNARE, as they are targets of the v-SNARE (Bonifacino & Glick, 2004) . VAMP and Syntaxin contain a transmembrane domain at the c-terminal end which allows membrane binding (Bonifacino & Glick, 2004). SNAP does not contain a transmembrane domain; however, they are bound to membranes through palmitoyl side chains formed through thioester linkages to cysteine residues located in the center of the molecule (Gonzalo, et al., 1999). SNAPs also contain two SNARE motifs, which are both used in SNARE complex formation to drive membrane fusion (Ramakrishnan, et al., 2012).

Table 1. *List of SNARE family proteins and their properties*. A list compiling the discovered SNARE proteins isoforms from the SNARE families: syntaxin, SNAP and VAMP. Isoforms are localized to different subcellular compartments, aiding in membrane fusion events within their respective compartment. Syntaxin and SNAP have common Q-SNARE motif structure while all VAMPs contain the R-SNARE motif.

Name	Locations	Synonyms	Type
Syntaxin1	PM	HPC-1	Qa
Syntaxin2	PM	Epimorphin	Qa
Syntaxin3	PM		Qa
Syntaxin4	PM		Qa
Syntaxin5	Go		Qa
Syntaxin6	TGN and Endosomes		Qc
Syntaxin7	EE and LE		Qa
Syntaxin8	EE and LE		Qc
Syntaxin10	TGN		Qc
Syntaxin11	TGN and LE		Qa
Syntaxin13	EE	Syntaxin12	Qa
Syntaxin16	TGN		Qa
Syntaxin17	ER		Qa
Syntaxin18	ER		Qa
SNAP-23	PM	Syndet	Qb and Qc
SNAP-25	PM		Qb and Qc
SNAP-29	Go and End	GS32	Qb and Qc
VAMP1	SV	Synaptobrevin1	R
VAMP2	SV	Synaptobrevin2	R
VAMP3	EE and RE	Cellubrevin	R
VAMP4	TGN and EE		R
VAMP5	PM		R
VAMP7	LE and Ly and PM	Ti-VAMP	R
VAMP8	EE and LE	Endobrevin	R

PM; Plasma Membrane, Go; Golgi apparatus, TGN; Trans Golgi network, EE; Early Endosome, LE; Late Endosome, ER; Endoplasmic Reticulum, END; Endosomes, SV; Secretory Vesicles, RE; Recycling Endosomes, Ly; Lysosomes

Four SNARE motifs are required to interact with one another to drive membrane fusion events via formation of a SNARE complex. A SNARE complex consists of three Q-SNARES and one R-SNARE (Cai, et al., 2007) which forms a twisted parallel 4-helical bundle which will zipper up the membranes (Hong, 2005). The energy generated from the formation of the four-helical bundle is hypothesized to catalyze the fusion process. Dissociation of SNARE complexes are driven by soluble N-ethylmaleimide-sensitive factor attachment protein (αSNAP) and N-ethylaleimide-sensitive factor (NSF) (Hong & Lev, 2014).

Unregulated SNARE complexes have been implicated in the highly-studied Parkinson's disease. When a SNARE complex is formed its dissociation must take place for membranes to fuse. In synapses α-synuclein mediates the dissociation of these SNARE complexes (Bonini & Giasson, 2005). Mutations in the α-synuclein gene mutate the protein causing it to aggregate rendering it incapable of unzipping the SNARE complex. When the dopamine containing vesicles do not fuse with the synapse, it is not released into the synaptic cleft and the dopamine neurotransmitter mediated action potential will not take place in the brain (Hunn, et al., 2015). The death of these neurons through this aggregation results in Parkinson's disease.

1.5 Impaired trafficking and resulting pathologies

Regulation of endocytosis, exocytosis and degradation pathways are important to maintain the health of an individual as exemplified in the afore mentioned diseases, type 2 diabetes and Parkinson's disease (Skach, 2000; Hunn, et al., 2015).

Cardiac-specific trafficking defects are still being investigated however there is evidence to implicate Brugada's syndrome to defective trafficking. Burgada's syndrome is a cardiac arrhythmia disease involving the altered expression of the sodium channel Nav1.5, and is characterized by extended conduction intervals and ST-segment elevation resulting in sudden cardiac death (Brugada, et al., 2014). Brugada's syndrome has been linked to mutations in the gene that codes for Nav1.5, however there is data to suggest that the impaired trafficking of Nav1.5 can also result in Brugada's syndrome (Hu, et al., 2009). In a clinical study performed in Japan some patients exhibiting Brugada's syndrome had a mutation in a novel tail anchored membrane protein called SLMAP (Ishikawa, et al., 2012).

1.6 Sarcolemmal Membrane Associated Protein

Sarcolemmal membrane associated protein, or SLMAP, is a novel class of tail anchored membrane proteins. It is encoded in chromosome 3p.13-21 in humans spanning approximately 122kbp and consisting of 24 exons (Guzzo, et al., 2004). Northern blot analysis indicated that the SLMAP gene codes for three

transcripts: 3.5 kbp, 4.5 kbp, and 5.9 kbp (Wigle, et al., 1997) which were revealed to be alternatively spliced and generated from a single locus. The three transcripts of SLMAP are translated into three isoforms: SLMAP1 (35 kDa), SLMAP2 (45kDa), and SLMAP3 (83-91kDa) each with their own unique methionine codon (Wielowieyski, et al., 2000). SLMAP3 have alternate transcription start sites in different exons resulting in one variant being significantly larger than the other (**Figure 2**). The SLMAP isoforms have their own unique variants due to alternative splicing of various exons within them which predict approximately 100 variants of the SLMAP protein. The 12 most common and characterized variants have been described in Figure 2 (Aken, et al., 2016). The isoforms show some tissue-specificity, SLMAP3 is expressed ubiquitously while SLMAP1 and SLMAP2 are expressed mainly in the myocardium and skeletal muscle (Wigle, et al., 1997).

Structurally SLMAP isoforms contain unique N-terminal sequences and c-terminal sequences (**Figure 2**). The N-terminal region of SLMAP3 contains an forkhead associated domain (FHA) and a Proline, Arginine, Serine, Threonine (PEST) rich region, which implicate SLMAP3 function in the cell cycle and microtubule formation (Guzzo, et al., 2004). The conserved c-terminal region for all three isoforms includes a leucine zipper domain and a transmembrane domain. The leucine rich coiled coil domain promotes protein-protein interaction through homo and heterodimerization (Guzzo, et al., 2004). There are two transmembrane domains of SLMAP, which are alternatively spliced to yield a TM1 or TM2 domain (Guzzo, et al., 2005). Each transmembrane domain in SLMAP localizes

to a separate subcellular compartment within the cell. Immunofluorescent analysis indicates both TM1 and TM2 localize to the endoplasmic reticulum, however only TM2 was shown to localize to the mitochondria (Byers, et al., 2009). SLMAPs share a structural homology with Syntaxin and VAMP which are also tail anchored proteins and, as mentioned, are involved in membrane trafficking and fusion (Nader, et al., 2012).

We demonstrated that SLMAP is involved in numerous cellular functions. In particular SLMAP3, the largest isoform, is a component of the microtubule organizing center (MTOC) and may serve a role in centrosomal functions (Guzzo, et al., 2004). SLMAP3 can also be localized to the centrosome based on staining with centrosome marker, γ-tubulin. This interaction appears to be through the FHA domain since its removal resulted in the decreased SLMAP3 localization to the centrosome (Guzzo, et al., 2004). The FHA domain has binding partners involved in spindle bipolarity and centrosome separation, therefore implicating SLMAP3 as an important regulator of cell cycle (Sueishi, et al., 2000). In support of this FACS analysis of cells overexpressing SLMAP3 showed an increase in cell growth compared to untransfected cells (Guzzo, et al., 2004).

SLMAP has also been implicated in myogenesis by playing a role myoblast fusion. Its expression is developmentally regulated during early skeletal myogenesis, and when, SLMAP was downregulated it inhibited the fusion of myoblasts into myotubes (Guzzo, et al., 2004).

SLMAP is also observed to be developmentally regulated within the heart with high expression in embryos at E9, E13 and E18 (Guzzo, et al., 2005).

Costaining of adult rat cardiomyocytes with SLAMP and SR markers, caveloin-3 and ryanodine receptor revealed a significant localization of SLMAP in t-tubule membrane and SR suggesting a potential role in EC coupling (Guzzo, et al., 2005). The c-terminal transmembrane domain allows SLMAP to target different areas of the cardiomyocyte suggesting that SLMAP plays a role in membrane organization (Guzzo, et al., 2004).

SLMAP has also been shown to play a role in intracellular trafficking. As noted earlier, SLMAP has been implicated in Brugada's syndrome. The mutated SLMAP expressed in patients exhibiting Brugada's syndrome resulted in the decreased trafficking of Nav1.5 to the cell surface (Ishikawa, et al., 2012). Cells expressing the mutated version of SLMAP underwent patch clamp analysis which revealed a significantly lower current density compared to Wt SLMAP. It was also observed siRNA targeting the mutant SLMAP gene rescued the trafficking defect of Nav1.5 and increased its movement from intracellular stores to the cell membrane (Ishikawa, et al., 2012).

SLMAP has also been implicated in the trafficking of GLUT4 in the *Tally Ho* mouse model: which when given a high glucose diet can develop type 2 diabetes. In this diabetic model, a significant increase in cytosolic but not cell surface GLUT4 was observed which is similar to human patients exhibiting type 2 diabetes. These diabetic mice also had elevated levels of SLMAP1 and SLMAP2 in both the cytosol and plasma membrane suggesting an association between SLMAP and GLUT4 (Chen & Ding, 2011). Intriguingly when *Tally Ho* adipocytes were treated with SLMAP siRNA, this resulted in decreased glucose

uptake implicating an impaired trafficking role of GLUT4 to the plasma membrane (Chen & Ding, 2011). This study concluded that the tail anchored membrane homology shared between SLMAP and SNARE's suggest SLMAP could be involved in fusion and trafficking of proteins such as GLUT4.

To further explore the role of SLMAP in cardiology and trafficking led us to create an transgenic (tg) mouse model with cardiac specific expression of SLMAP1. Hematoxylin and eosin staining of 6-week-old transgenic mouse hearts showed a significant increase in vesicle formation within the myocardium which directly correlated to the level of SLMAP1. SLMAP1 overexpression also affected cardiac membrane structures, ER and SR, causing dilation and uneven membranes to develop (Nader, et al., 2012). The protein expression of calcium signalling proteins localized to the SR (RyR2, Serca2a and CSQ) were dramatically decreased in the tg mouse hearts, thus implicating SLMAP1 as a modulator of EC coupling by affecting intracellular calcium homeostasis (Nader, et al., 2012).

Further experimentation on these tg mice revealed that the large vesicles were early endosomes which expressed the early endosome markers Rab5 (Dewan, 2016). We also noted a significant upregulation of GLUT4 protein, without an increase in its transcript levels, suggesting it was upregulated via a mechanism involving intracellular recycling (Dewan, 2016). In support of this we observed a co-localization of the recycling endosome marker (Rab11) in compartments present on the enlarged vesicles (Rehmani, et al., 2016). These results signify that increased expression of SLMAP1 led to significant changes in

intracellular trafficking pathway which ultimately affected the expression of GLUT4 on the plasma membrane.

Inherently animal models are important tools in deciphering *in-vivo* function. Exploring the *in-vivo* overexpression model for SLMAP has aided in understanding its role in the mouse myocardium. Hence a knockout model for SLMAP could aid in further establishing its role in the mammalian system. A global knockout of SLMAP resulted in embryonic lethality in mice (Tuana, unpublished) therefore it was proposed that by using the Cre-Lox system we could control the spatial and temporal nature of the knockout preventing embryonic lethality.

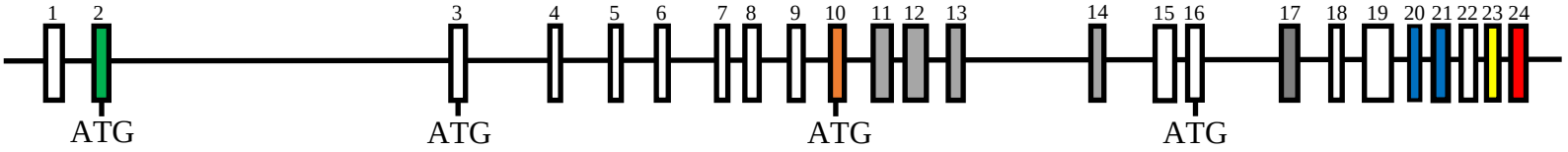

SLMAP3 (95-80 kDa)

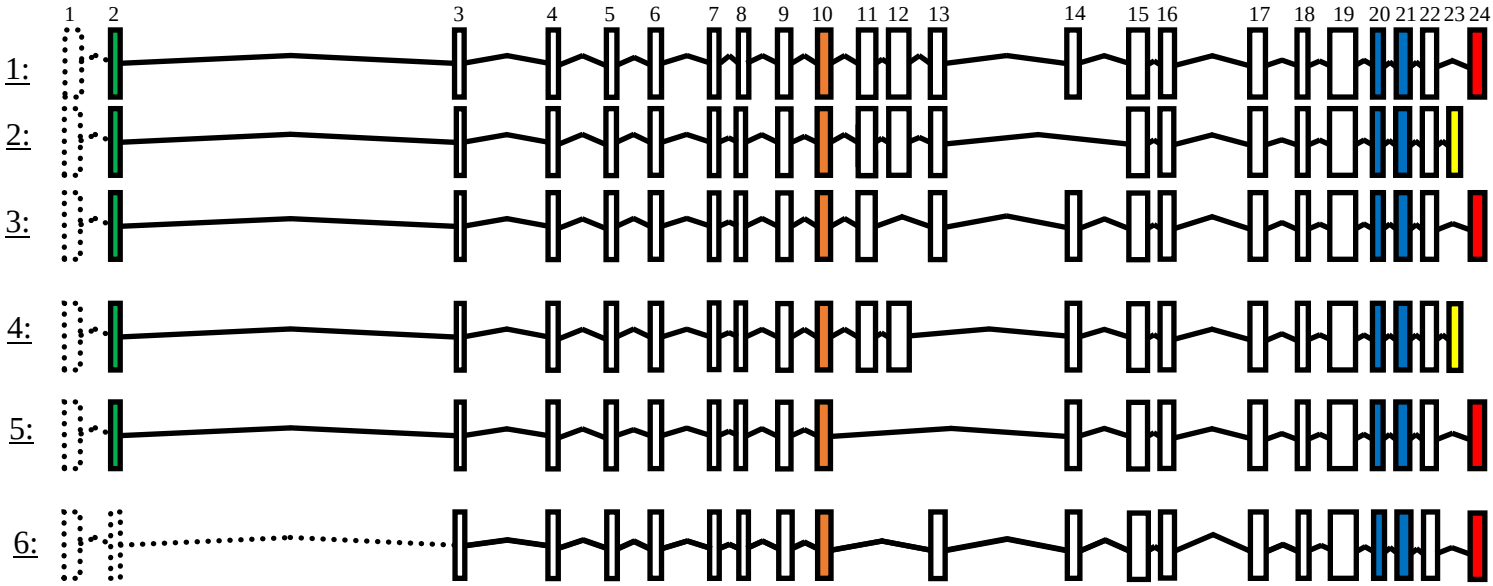

SLMAP2 (45 kDa)

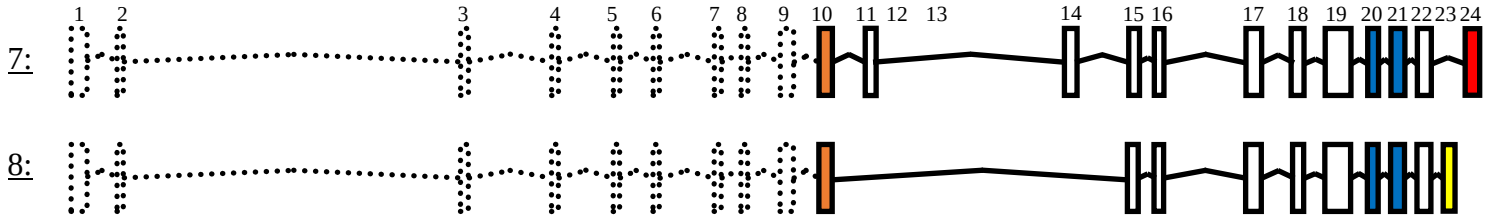

SLMAP1 (35kDa)

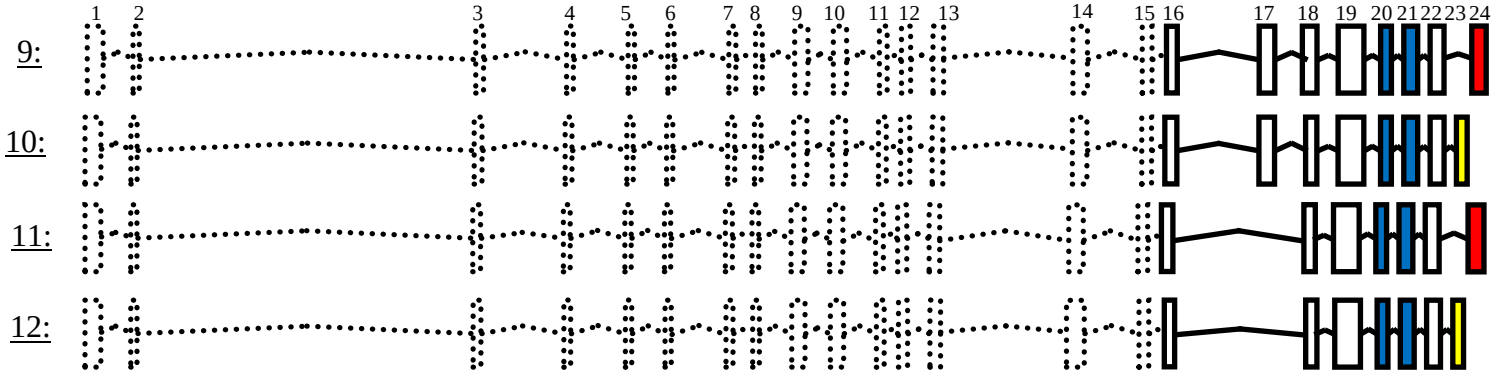

Figure 2. *Genomic organization of mouse SLMAP gene.* The SLMAP gene consists of 24 exons (black) and numerous intron sequences (thin lines) equating to approximately 122kbp of DNA (top). Alternative splicing of SLMAP gene results in three distinct isoforms that expressed in myocardium; SLMAP1 (35 kDa), SLMAP2 (42 kDa), or SLMAP3 (83-91 kDa). SLMAP3, SLMAP2, and SLMAP1 isoforms are determined by alternate first exons initiated at exon 2/3, exon 10, or exon 16 respectively. Further diversity is in SLMAP is generated due to additional alternative splicing of exons 11, 12, 13, 14, 17 (grey) and the mutually exclusive exons 23 and 24 which code for one of two transmembrane domains, TM1 (yellow) or TM2 (red). Exon 2 (green) codes for forkhead associated domain (FHA) which is only present in SLMAP3. Exon 10 (orange) translates a Proline, Glutamic acid, Serine, Threonine domain which is only present in SLMAP3 and SLMAP2. Exon 20 and 21 (blue) code for coiled-coil regions and along with transmembrane domain is present in all three isoforms. Copyright (2017) of Balwant Tuana laboratory at the University of Ottawa.

1.7 Conditional knockout mouse model using the Cre-Lox System

1.7.1 Cre-Lox System

The Cre-Lox system is site-specific recombination system used to modify DNA through a system derived from the P1 bacteriophage. The P1 bacteriophage infects *E.Coli* trough a mechanism involving site-specific recombination. This site-specific recombination was used to remain a plasmid in the lysogenic state. (Hochman, et al., 1983). Further research and experimentation revealed recombination was due to a synergetic role of recombinase, Cre, and a 34bp sequence, loxP (Sauer & Henderson, 1988). LoxP sites 34 bp sequence is broken down into 13-bp inverted repeats with an 8bp nonpalindromic sequence in between these repeats to provide orientation to the overall sequence (Missirlis, et al., 2006). Cre (Causes REcombination) was observed to bind to a loxP site and recombine the phage's genome to the hosts loxP sequence to maintain the lysogenic state (Austin, et al., 1981). The 13bp repeats serve as binding domains for the cre enzyme, which allow recombination to take place (Hoess, et al., 1986). The simplicity of cre with no additional requirements for the recombination such as cofactors or accessory proteins to regulate its expression, and loxP site being non-endogenously expressed in mammals, allows the Cre-Lox system to be an ideal candidate for genetic engineering in cells and animal models.

Eukaryotic model must undergo genetic modification to contain a loxP site at the sequence of interest. There needs to be two loxP sites in the region of interest to cause recombination (Branda & Dymecki, 2004). The orientation of the two loxP sites determines the type of recombination to take place (Kuhn &

Torres, 2002). The two loxP sites that are oriented forward will result in the excision of a sequence between the loxP sites (Wu, et al., 2007). LoxP sites are opposite each other result in the inversion of the sequences (Grégoire & Kmita, 2008). Finally, if two loxP sites are on different strands, the strands will translocate to one another causing a hybrid strand (**Figure 3**) (Hamilton & Abremski, 1984). Flanking a region of interest with loxP sites determines the type of genetic modification that takes place in the model ranging from affecting gene regulators to causing small or large genomic deletions (Orban, et al., 1992). When loxP sites are added to flank a region, these regions are then referred to as floxed.

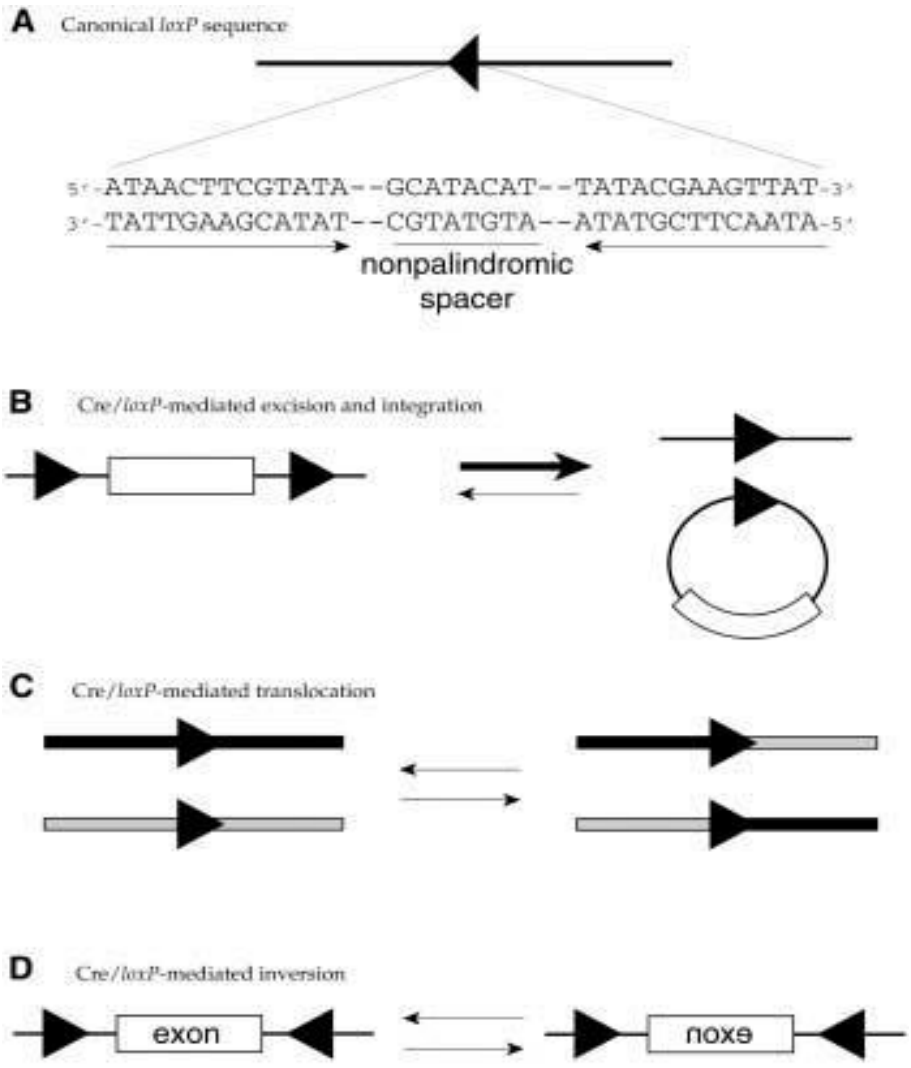

Figure 3. *Orientation of LoxP sites are essential for cre mediated recombination*. A) LoxP sites sequence contain 34 bp sequences. B) Cre causes recombinase to take place by recombining the sequences in between the floxed region, excising them and then recombining the excised strand. C) LoxP sites placed on different strands of DNA will result in translocation causing hybrid strands of DNA. D) LoxP sites on the same DNA strand and are oriented opposite to each other result in inversion of the flanked region. Figure reprinted with permission from (Kuhn et al, 2002). Copyright (2002) Springer.

1.7.2 Cre: structure and function

Cre recombinase is a quaternary protein structure consisting of 343 amino acids and form two distinct domains. It creates 5 alpha helical segments, two of them form a major groove which directly interact with the loxP DNA (Guo, et al., 1997). The active site of the enzyme is found on the carboxyl terminal domain, amino acids 132-341 (Guo, et al., 1997).

The active site is made up of conserved residues arginine, histidine, arginine, and nucleophilic residues tyrosine and tryptophan. Tyrosine acts as a nucleophile to form a covalent 3'-phosphotyrosine linkage to the DNA substrate. Tryptophan forms a hydrogen bond to a scissile phosphate; this reaction cleaves DNA and frees the 5' hydroxyl group (Guo, et al., 1997).

1.7.3 Fusion of Cre with hormone binding domains and promoters allows spatial and temporal control of recombinase activity

For several years studies were done to render intracellular proteins activity hormone-dependent by fusing them with a hormone binding domain (HBD) (Picard, 1993). The HBD human estrogen receptor (EsR) has been extensively utilized as presence of endogenous EsR is partial in various cell types (Tora, et al., 1989). This allows the control of activity of protein fused with ER by administering the EsR stimulating ligand 17β-oestradiol, which is cost-effective and easy to administer (Littlewood, et al., 1995). However, noticeable drawbacks for this expression were observed particularity in an *iv-vivo* model in which the

EsR could be transiently activated by endogenous estradiol hormone expression (Littlewood, et al., 1995). These drawbacks were overcome with the development of a mutated EsR, known as MER. These MER receptors were no longer able to bind endogenous estrogen or 17β-oestradiol but only to estrogen analogs, such as tamoxifen (Littlewood, et al., 1995).

Cre was fused with MER, resulting a Cre-Mer recombinase that is only activated in the presence of tamoxifen (Metzger, et al., 1995). The Cre-Mer is anchored to the cytoplasm by forming a complex with heat shock 90 proteins (hs90) (Scherrer, et al., 1993). When tamoxifen is added heat shock 90 proteins dissociate and Cre-Mer is translocated to the nucleus and recombination takes place (Verrou, et al., 1999). Cre-MER activity analysis revealed incomplete recombination events and displayed a level of background activity pre-tamoxifen administration (Zhang, et al., 1996). Due to this a double MER ligand Cre, MERCreMER, was developed. The hs90 proteins would increase MER anchoring to the cytoplasm thus reducing background activity. Tamoxifen-induced activity was measured to be superior to its single ligand counterpart in detection, function and activity (Verrou, et al., 1999). Therefore, the MERCreMER recombinase is the most efficient model for temporal recombination in a cre-lox model.

Finally, to mediate tissue specific expression a promoter can be engineered on to the cre gene. Promoter sites initiate transcription of DNA and specific promoters result in tissue-specific expression (Gagniuc & Ionescu-Tirgoviste, 2012). Two factors need to be addressed in order to engineer a promoter onto DNA construct; 1- the cells affected by promoters and 2- the

temporal expression (Davis, et al., 2012). To generate a cardiac-specific knockout model the α-myosin heavy chain (α-MyHC) promoter or β-MyHC can be engineered onto the MerCreMer to drive recombinase activity in cardiomyocytes (Jones, et al., 1994; Rindt, et al., 1993). The α-MyHC is preferred to β-MyHC due it high specificity to cardiomyocytes and higher transcriptional activity (Davis, et al., 2012). By using the α-MyHC-MerCreMer model we can control the temporal and spatial nature of the recombination of our flox-DNA (Sohal, et al., 2001).

The limitation to using tamoxifen in α-MyHC-MerCreMer mouse model is that tamoxifen results in transient cardiomyopathy, characterized by a reduction in systolic function (Hall, et al., 2011), and evidence of DCM following cardiac remodeling (Buerger, et al., 2006). The mechanism through which tamoxifen causes cardiomyopathy is largely unknown; but post-tamoxifen inspection demonstrated the upregulation of apoptotic markers, decreased metabolism, increased stress markers, and increased cardiomyocyte death (Koitabashi, et al., 2009; Bersell, et al., 2013). However, this myopathy is transient; cessation of tamoxifen treatment prompts heart function to return to normal (Hall, et al., 2011). Dosage of tamoxifen must be calibrated as studies have shown that less than minimum results in little to no recombination and more than maximum results in mortality (Kiermayer, et al., 2007). There are two main methods of tamoxifen administration: intraperitoneal (I.P) injections and tamoxifen diets (Davis, et al., 2012). I.P injections are preferred due to much greater accuracy in the dose of tamoxifen given and a shorter incubation time (Andersson, et al., 2010). A protocol that utilized 5-day I.P injections with 20 μg of tamoxifen/g of

animal was insufficient for floxed gene knockdown and a dose of 80 µg/g resulted in 60% mortality in the α-MyHC-MerCreMer mice (Koitabashi, et al., 2009). The most effective dosage has been shown to be 30 µg/g of tamoxifen per gram of animal. This dosage resulted in the least amounts of fibrosis and cardiac dysfunction whilst maintaining high recombination efficiencies (Bersell, et al., 2013; Zhao, et al., 2016)

1.8 Statement of problem

SLMAP is novel tail anchored membrane protein that is highly expressed and developmentally regulated and is therefore thought to play significant role in the myocardium. Overexpression of SLMAP1 in postnatal myocardium has shown to cause significant membrane remodeling (vesicle expansion, ER/SR membrane dilation), and downregulation of calcium signalling proteins. This vesicle expansion led us to discover that they were enlarged early endosomes and were directly involved in upregulating GLUT4 through a recycling mechanism. Therefore, I believe SLMAP plays a role in intracellular trafficking impacting the function of myocardium

In this thesis, I developed an *in vivo* mouse model for cardiac specific knockout of SLMAP in postnatal myocardium to determine its function and establish its role in vesicle trafficking. I hypothesize that *SLMAP deficiency will impact the function of postnatal myocardium by affecting membrane structures and protein trafficking.*

To assess my hypothesis, the following objectives were explored:

1. To establish cardiac specific SLMAP deficient mice:

   I developed an SLMAP knockout mouse model using the cre-lox system and extensive breeding strategy described in Materials and Methods.

2. To assess the role of SLMAP deficiency on cardiac structure and function

   I will use transthoracic echocardiography (ECHO) to assess wall thickness, LV diameter and LV performance.

3. To determine if a deficiency of SLMAP impacts vesicle trafficking

SLMAP expression has been linked to vesicle trafficking. I evaluated the expression of endosomal recycling proteins in SLMAP deficient model via biochemical analysis.

Chapter 2: Materials and methods:

2.1 Creating a transgenic flox-SLMAP mouse line

A targeting construct vector for SLMAP was developed using neomycin insertion cassette. Exon 3 of the mouse SLMAP gene was chosen to flank with two loxP sites. The vector was microinjected into embryonic stem cells and implanted into C57BL/6 blastocysts. The founder (F0) flox-SLMAP animals were confirmed through genotyping and were maintained through breeding with C57BL/6 mice.

The α-MyHC-MerCreMer mice are a core component to generate the SLMAP knockout model. α-MyHC-MerCreMer mice were generously donated by Dr. Mona Nemer and were maintained by breeding with C57BL/6.

2.2 Generating and genotyping the SLMAP knockout model

a) *Breeding strategy*: Extensive breeding needs to take place to generate a cre-lox animal model that can knockout SLMAP. The breeding is separated into three different generations, F0, F1, and F2 (**Figure 4)**. In F0 breeding, flox-SLMAP and α-MyHC-MerCreMer mice were crossed with Wt C57BL/6 mice to maintain the lines and further generate F1 and F2 animals.

F1 breeding is utilized in the generation of knockdown (KD) and homofloxed animals. The knockdown animals breeding pair consisted of a flox-SLMAP crossed with α-MyHC -MerCreMer resulting result in 25% of the offspring's to be knockdown animals (heterozygous flox-SLMAP and Cre positive). The homofloxed breeding pair consisted of flox-SLMAP crossed with flox-SLMAP to result in 25% homozygous (two alleles) flox-SLMAP animals. Generally, F1

breeding results in an intermediate line that is utilized for breeding to generate the knockout (KO) animal. However, KD animals are also used for studies as one allele of SLMAP will be cleaved.

Finally, the F2 breeding results in the generation of KO animals. This is achieved by homoflox-SLMAP animals crossed with the KD animals resulting in 25% of offspring containing homo-flox SLMAP and Cre, the prerequisite genetic material to knockout SLMAP.

All animals were handled in accordance to protocols approved by the Institutional Animal Care and Use Committee.

b) *Genotyping*: Mice were genotyped by extracting genomic DNA from ear clips by boiling for 10 minute at 95^0C in 180µL of 50mM NaOH per ear. DNA solution was then neutralized using 20µL of 1M Tris-Cl pH 8.0. SLMAP KO/KD mice were identified by polymerase chain reaction (PCR) using DreamTaq Green PCR Master Mix 2x (Thermoscientific) for the PCR mix. To determine flox-SLMAP or wt-SLMAP the forward F2 primer was (5`-CCT GGA GAG CCT CCG TGT GAG T- 3') sequence and reverse R2 primer (5`-GTC AAC TGC CCA ATG TAC AGA AAT AGT AAG -3`) targeted loxP site 1. This resulted in a PCR product of ~424bp or ~282bp having either flox-SLMAP or wildtype-SLMAP. To determine $Cre^+$ animals forward primer Cre-F (5'-ACG ACC AAG TGA CAG CAA TG-3`) and reverse primer Cre-R (5'-AAC CAG CGT TTT CGT TC-3'). PCR product in Cre^+ animals resulted in bands that were ~425bp. PCRs were visualized by Red Safe (Sigma) staining on a 1% agarose gel.

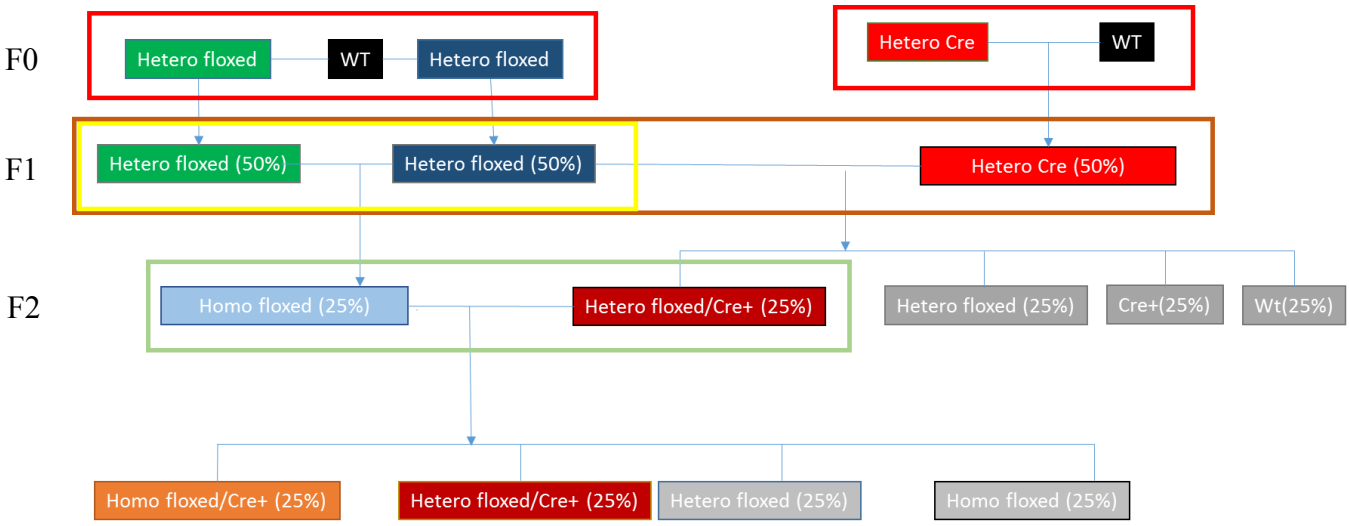

Figure 4. *Breeding diagram for α-MyHC-MerCreMer/Flox-SLMAP animals.* Breeding diagram to produce mice that contain floxed SLMAP alleles and cre. F0 generation is used to label the heteroflox-SLMAP (green/dark blue) and hetero-cre (red) mice. Each heterofloxed and hetero-cre mouse are maintained separately with Wt. The separated heteroflox mices' offspring were bred together to generate the homofloxed animal (blue), labelled in the F1 generation. Additionally the F1 generation labels the production of knock down (KD) (Dark red; heterofloxed and hetero-cre) after breeding a hetero-cre mouse with a heterofloxed mouse. F2 generation highlights the generation of KO (Orange; homofloxed and cre) mice by breeding homofloxed animal with a KD animal. Copyright (2017) of Balwant Tuana laboratory at the University of Ottawa.

2.3 Activation of Cre and assessing recombination of flox SLMAP

Tamoxifen (Sigma) is administered into animals to activate MerCreMer to cause a cleave floxed regions. 500 µg of Tamoxifen was dissolved into 10 ml of peanut oil (Sigma), aliquoted into 10 different tubes and frozen at -20ºC for long term storage. Tamoxifen was injected intraperitoneally in 5-week-old animals at a dose of 30 µg tamoxifen/g of animal for 3 days. Tamoxifen treated hearts were excised and clipped to be analyzed by PCR genotyping as described above. The primers used were forward primer F2 (5`-CCT GGA GAG CCT CCG TGT GAG T- 3') and reverse primer R1 (5'-GGA GAG ACT ATC ACA GCC ACA GGA-3'), coding for sequences between loxP sites; exon 3 and intron sequences.

2.4 Protein isolation from mouse heart

Hearts of adult mice were collected after CO_2 euthanasia, and immediately frozen in -80^{0}C. Each heart was later washed with ice-cold 1X phosphate buffered saline (PBS), and homogenized using Fisher handheld Maximzer homogenizer in ice-cold lysis buffer (1mM ethylene glycol tetraacetic acid (EGTA), 1 mM ethylenediaminetetraacetic (EDTA), 20 mM Tris base, 1% Triton, 150 mM sodium chloride, 1X complete mini EDTA-free protease inhibitor cocktail (Roche), and 1X PhosSTOP (Roche). The suspension was centrifuged for 15 min at 12,000g to separate the proteins from cell debris. The supernatant containing protein was collected in eppendorf tubes and stored in freezer at -80ºC. In immunoblotting experiments, proteins from each heart were used in a single lane of 10% sodium dodecyl sulfate polyacrylamide gel electrophoresis (SDS-PAGE).

2.5 SDS-PAGE and Western blots

For western blotting experiments, 30 µg of protein was loaded in each well of a 5-15% SDS-PAGE gel. The gels were transferred overnight on a polyvinylidene fluoride (PVDF) membrane (Bio-Rad) in a buffer containing 25 mM Tris, 190 mM Glycine, and 20% methanol. All membranes were blocked at room temperature for 1-hour in Tris-buffered saline (TBST) containing 1 M Tris, 290 mM NaCl, 0.1% Tween 20, pH 7.4, and 5% non-fat dry milk. Primary antibodies were incubated overnight at 4^{o}C with 5% bovine serum albumin (BSA). Membranes were washed 5 times for 5 min each in TBST prior to adding the appropriate horseradish peroxidase labeled secondary antibody (Jackson) in a 1:10,000 dilution in TBST with 5% non-fat dry milk. Membranes were shaken slowly at room temperature for 1-hour while incubating with secondary antibody followed by 5 washes for 5 min each with TBST. Membranes were treated with BioRad western blotting kit (BioRad) and developed using ChemiDoc machines. Bands were quantified by densitometry using Image Lab software v.4.0.1 (Bio-Rad). Membranes were stripped (25 mM glycine, 10% SDS and pH 2.2 in dH_2O) and reprobed with different antibodies. All primary antibodies which were used are indicated in table 2 (below) along with corresponding dilutions.

Table 2. *List of antibodies used in this study.* All antibodies used in this study are listed with the corresponding distributor, catalog number, and dilution used for each application

Antibody	Manufacturer	Application (Dilution)
SLMAP (anti-rabbit)	NovusBio (NBP1-81397)	IF (1:100), WB (1:1000)
SLMAP (anti-mouse)	Abnova (H00007871-M08)	IF (1:100)
α-Tubulin	Abcam (ab176560)	WB (1:5000)
EEA1	Cell Signalling Technology (3288)	IF (1:100), WB (1:1000)
VAMP2	Abcam (ab3347)	IF (1:100), WB (1:1000)
Syntaxin-4	Abcam (ab77037)	IF (1:100), WB (1:1000)
SNAP23	Abcam (ab3340)	IF (1:100), WB (1:1000)
RABEP1/Rabaptin-5	Proteintech (14350-1-AP)	IF (1:300), WB (1:5000)

2.6 Quantitative PCR

Total mRNA from mouse hearts was extracted using the SYBR green 2x QPCR mix (Roche). The concentration and purity of the obtained mRNA was determined by measurement of 260/230 nm absorbance ratio and 280/260 absorbance ratio -(Bustin, 2002) using NanoDrop 2000 UV-Vis Spectrophotometer (Thermo Scientific). RNA was used as a template to generate cDNA using SuperScript II reverse transcription protocol following the manufacturer's guidelines (Invitrogen). Equal amounts of cDNA were utilized in real-time PCR using primers for SLMAP3 cDNA (SLPN-F: 5'-GGA ATT CGA TGC CGT CAG CCT TGG C -3', 558-R: 5'-TTG CTC GTC TTG TGA TCA AAC CAG -3'), total SLMAP cDNA (GTY-F: 5'-GAA AAG CCT ATC GAA ATC AAG TTG-3', GTY-R: 5'-ACC TTC TTA AGC TCT TCT TGC AAA G-3') and 18S Ribosome (forward: 5'-AAT ACA TGC CGA CGG GCG CT -3', Reverse: 5'AGT GGG TAA TTT GCG CGC CT-3'). Fold change was calculated using the ΔΔCt method.

2.7 Echocardiography

All echocardiographic analysis was done using the VEVO 2100 system (VisualSonics). Adult mice were anesthetized using 2% isoflurane and strapped onto a heated pad, facing upwards exposing the thoracic cavity. 40MHz probe was used to capture short axis B-mode and M-mode images of the left ventricle. VEVO 1.6 software was utilized for measuring LV wall thickness and inner diameter in diastole and systole.

2.8 Isoproterenol Delivery

Isoproterenol (Sigma) delivery was mediated through the subcutaneous implantation of miniosmotic pumps (2001D Alzet) in 8-week-old mice. 0.9% saline or Isoproterenol, dissolved in 0.9% saline, was delivered at a rate of 30 µg/g/d per animal. Cardiac function was analyzed through echocardiography before pumps were implanted and after 7 days. After a week of isoproterenol administration, animals were euthanized and hearts were collected for protein or histological analysis.

2.9 Histological analysis

Hearts that were iso-treated were extracted from animals and fixed using 10% Neutral Buffered Formalin (Fischer). After fixing for 48 hours, hearts were sectioned 4 µm longitudinally per section. Sectioned hearts were stained with Hematoxylin and Eosin to visualize the myocardium.

2.10 Statistical Analyses

All comparisons between wildtype and knockdown or knockout groups were analyzed using two-tailed Student's T-test. If all three groups were analyzed ANOVA was utilized to determine significance. All values and points on graphs represent mean values obtained from multiple experiments. All error bars presented in graphs are represented using the standard error of the mean. All sample size values (n) represent biological replicates (different hearts for westerns or ECHO).

Chapter 3: Results

3.1 Characterizing the SLMAP KD, KO and Wt mice

To knockout the SLMAP gene using a Cre-Lox system, we chose to flank exon 3 with LoxP sites (Guzzo, et al., 2004). We hypothesized that cleaving exon 3 would result in a frameshift mutation affecting all downstream exons and thereby knockout all three isoforms of SLMAP (**Figure 5A)**. This gene was referred to as 'flox-SLMAP'. Heterozygous and homozygous flox-SLMAP mice were generated as detailed in the material and methods section. Similarly, α-MyHC-MerCreMer lines were generated as detailed in the material and methods section. Flox-SLMAP animals were crossbred with α-MyHC-MerCreMer to generate an animal which would contain both a flox-SLMAP and cre transgene, therefore containing the genetic potential to undergo a knockout (KO) or knockdown (KD) of SLMAP (Ayadi, et al., 2011).

PCR genotyping was utilized on ear clippings from individual animals to determine the presence of loxP and cre in each animal. Primers F2/R2 were used to locate loxP site 1, located upstream of exon 3, as shown in the mechanism in Figure 5A. The floxed SLMAP band was 424 bp in length, whereas wildtype was 282 bp in length (**Figure 5B)**. Lanes labelled Homo were represented by one band at 424bp which signified a homo-floxed animal as both SLMAP alleles were flanked with loxP sites. Lanes labelled Wt signified a wildtype (Wt) animal; a band present at 282 bp indicating SLMAP allele did not contain the loxP site. Finally, two bands in each lane, one at 424bp and one at 282bp were labelled as

Het as it signified an heterfloxed animal; one flox-SLMAP allele and one wildtype.

The α-MyHC-MerCreMer transgene was detected similarly via PCR genotyping except with primers CreF/CreR. They elongate a sequence in the cre gene that is approximately 425bp as shown in a mechanism in Figure 6A. A lane labelled Cre^{+} presented a 425bp band representing a cre positive animal (**Figure 6B**).

If an animal is suspected to contain both genes, PCR genotyping is carried out using both sets of primers independently to detect presence of loxP and cre gene i.e. their KD or KO designation. Each lane in Figure 7 represents an individual mouse. A KO lane contains two copies of flox-SLMAP (one band at 424bp) and the cre transgene, characterizing a KO animal. The KD lane contained one copy of flox-SLMAP (424 bp), one copy of wt-SLMAP (284b bp) and the cre transgene were characterized as KD animals. Finally, the Wt lane had one transgene or none represents a wildtype animal because both a flox and a cre are essential for a cleavage to take place (Kuhn & Torres, 2002).

A.

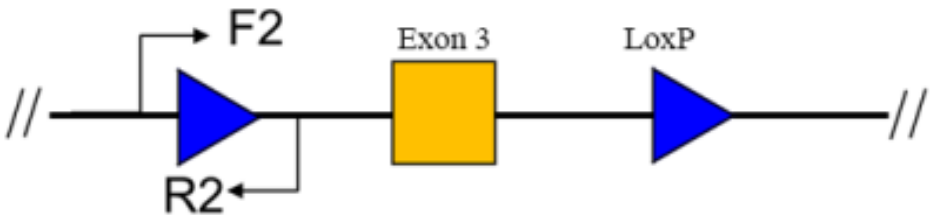

B.

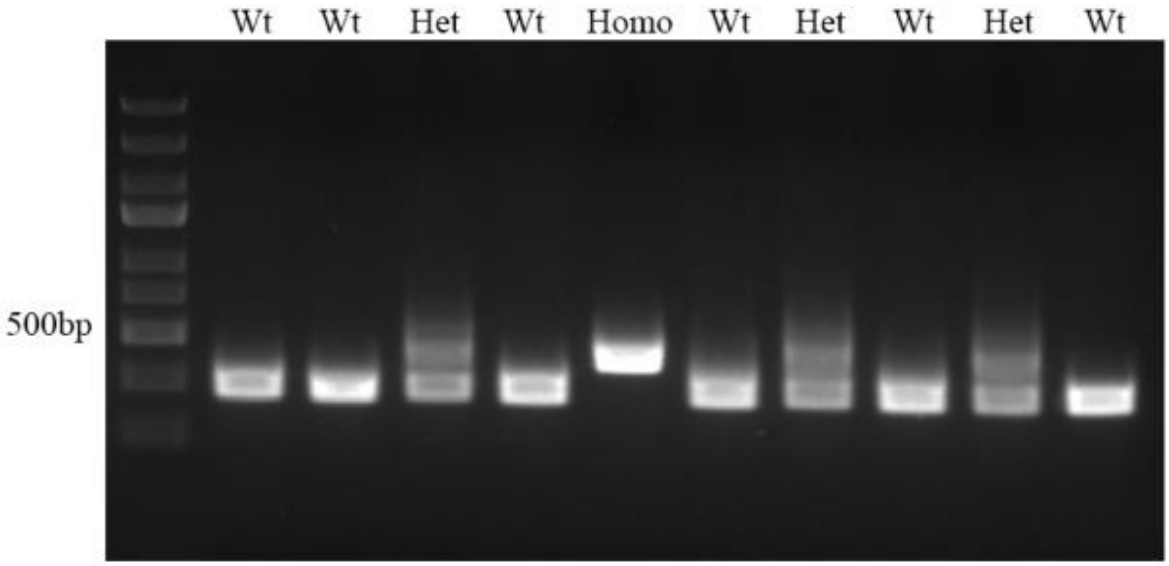

Figure 5. *Genotyping of hetero and homo Flox-SLMAP mice using primers F2/R2. A)* The primers F2/R2 target LoxP site 1. *B)* F2/R2 primers determine animals that are homofloxed, heterfloxed or wildtype. Upper bands signified flox-SLMAP (424bp), while lower bands signified wildtype SLMAP (280 bp). Homo lanes contained one flox-SLMAP band. Wt lanes contained one wildtype SLMAP band. Het lanes contained two bands, one flox-SLMAP and one wildtype SLMAP. Copyright (2017) of Balwant Tuana laboratory at the University of Ottawa.

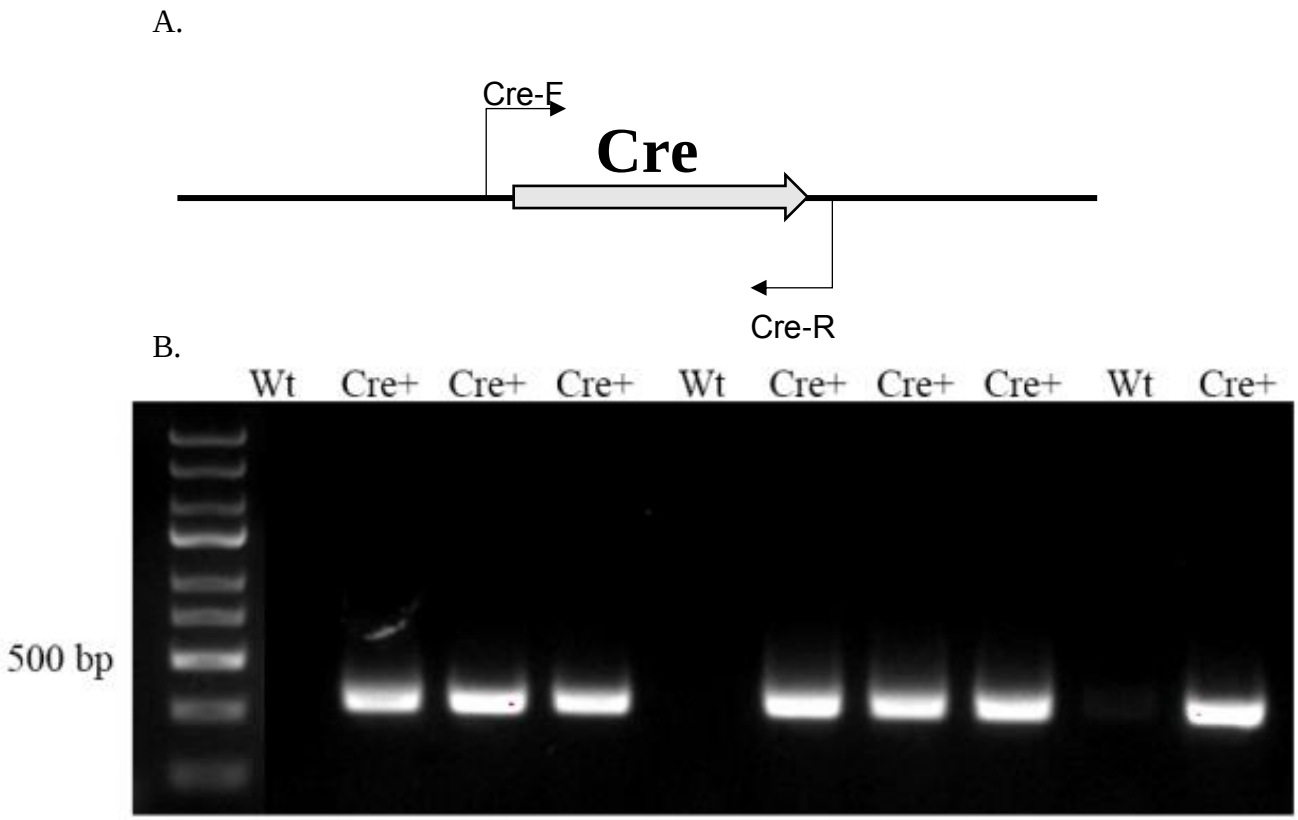

Figure 6. *PCR genotyping of* α-MyHC-*MerCreMer using primers Cre-F/Cre-R distinguishes Cre positive and Cre negative animals. A)* Mechanism on Cre-F/Cre-R primer targeting *B)* PCR genotyping confirming the presence of Cre (425bp) in animals using the primers Cre-F/Cre-R. Lanes containing a band are labelled Cre+ and empty lanes are labelled Wt.

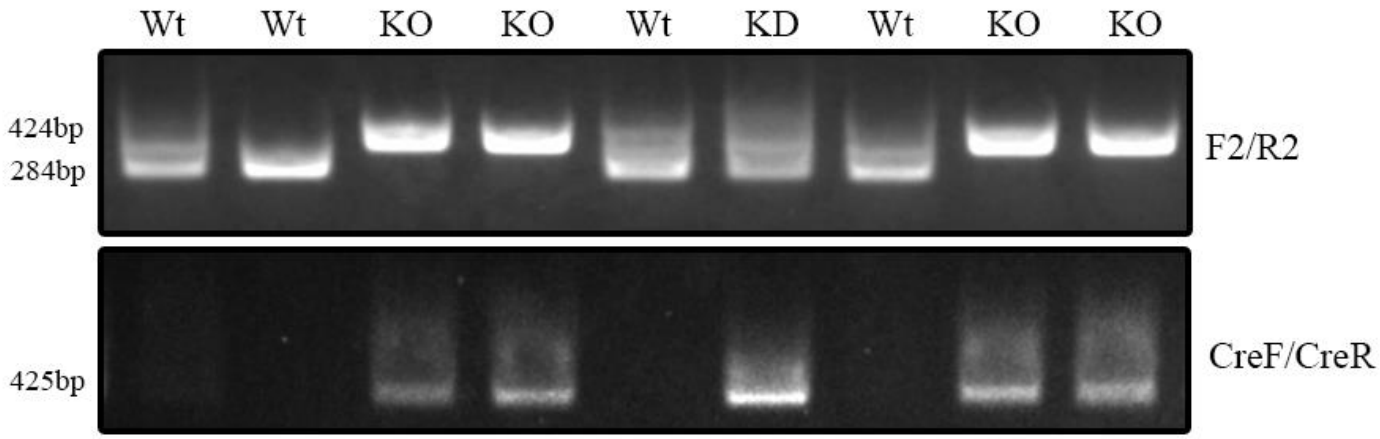

Figure 7. *Knockdown and knockout animals contain at least one Flox-SLMAP and the Cre gene.* KO lanes contained homofloxed SLMAP band and cre. KD lane contained heterofloxed SLMAP and cre. Wt lanes contained only one transgene or neither. Copyright (2017) of Balwant Tuana laboratory at the University of Ottawa.

3.2 Activation of α-MyHC-MerCreMer with tamoxifen results in the cleavage of flox-SLMAP region

After genotyping the animal that contains both flox-SLMAP and α-MyHC-MerCreMer I wanted to determine if excision of the flox-SLMAP region (exon 3 and surrounding introns) would take place after cre is activated through administration of tamoxifen. As mentioned earlier tamoxifen administration via intraperitoneal injections (I.P.) is the most effective method for inducing cre activation (Sohal, et al., 2001). Studies have shown that by administering 30 µg/g of tamoxifen for 3 days' results in the highest recombination efficiency, therefore our studies utilize the 30 µg/g for 3 days protocol (Bersell, et al., 2013). After tamoxifen treatment, KD and Wt hearts were analyzed through PCR amplification using primers F2/R1. These primers elongate the sequence between the two loxP sites, as shown in the mechanism in Figure 8A. Excision of the floxed region reduces it to 400bp while the unaltered SLMAP allele remains 1400bp in length (**Figure 8A**). Lanes labelled KD had two bands (one altered and one unaltered) while Wt lanes had only one band (**Figure 8B)**. Therefore, the activation of α-MyHC-MerCreMer via tamoxifen resulted in the removal of flanked region, including exon 3 from the flox-SLMAP gene.

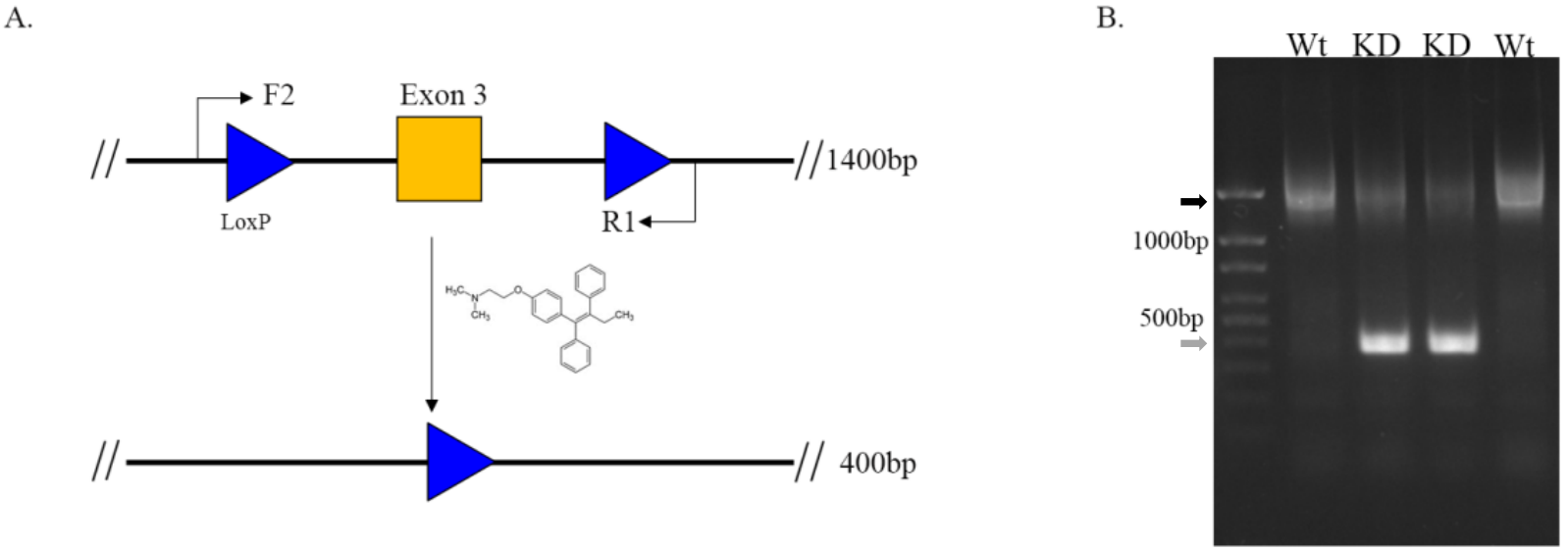

Figure 8. *Administration of tamoxifen results in cleavage of floxed SLMAP sequence.* A) Schematic showing cleavage of exon 3 in a KD animal after treatment with tamoxifen B) PCR genotyping of animals treated with tamoxifen using primers F2/R1. Wt lanes indicate unaltered SLMAP which results in1400 bp band. KD lanes result in two bands being present, cleaved SLMAP band (400bp; grey arrow) and an unaltered SLMAP gene (1400bp; black arrow).

3.3 SLMAP3 protein was knocked down and out animals

I then wanted to verify a decrease in the protein levels of SLMAP in KD and KO animals. Adult mice that I genotyped KD, KO or Wt were tamoxifen treated and left for a minimum of three weeks. Myocardial protein expression was analyzed by western blotting with anti-SLMAP and anti-tubulin.

The animals designated KD had a significant reduction in the expression of SLMAP3 relative to the Wt (-45.81% ± 9.581%, $p<0.001$, $n=6$) (**Figure 9**). This correlates with our assumptions that cleavage of one SLMAP allele results in approximately half on the SLMAP being decreased in the KD animals. In the KO animals, a complete knockout of SLMAP3 was observed (**Figure 10A**).

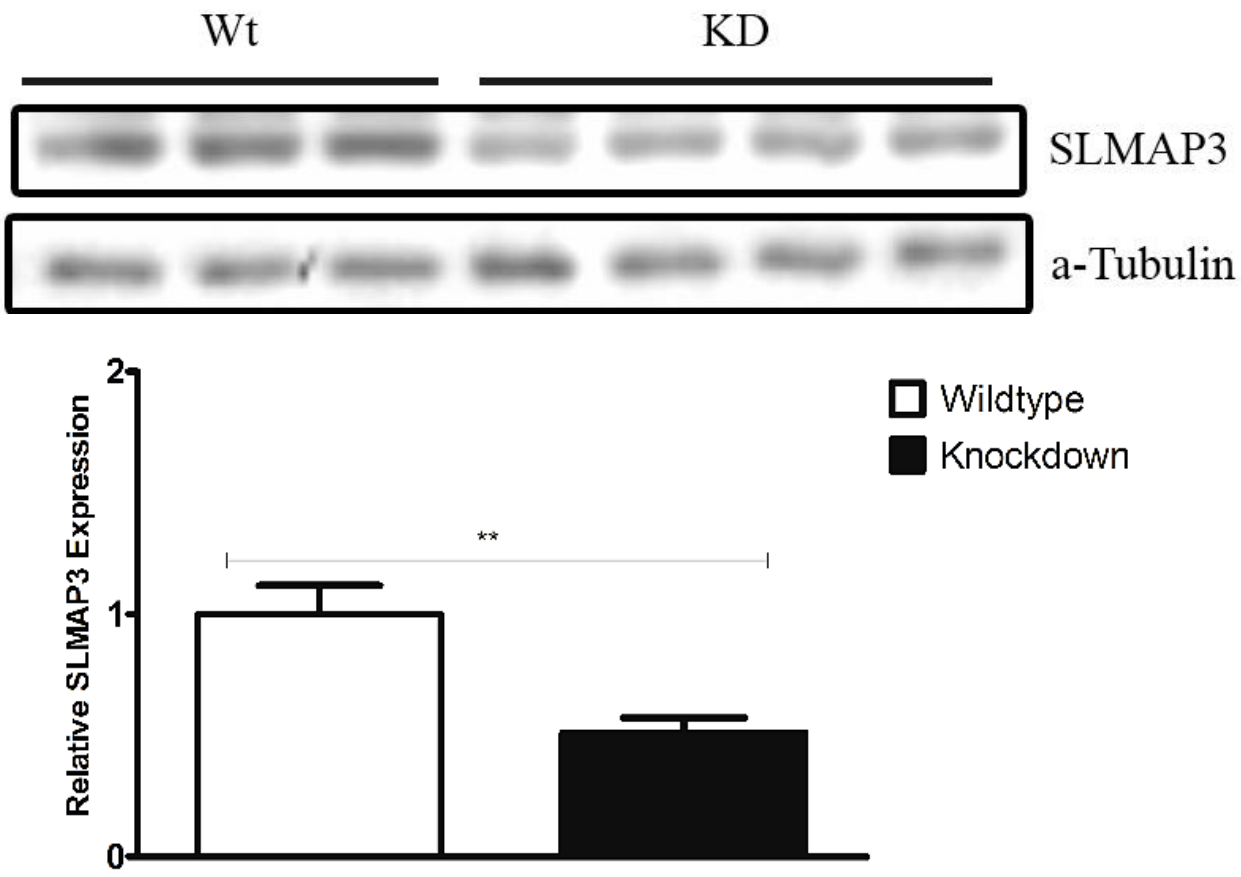

Figure 9. *SLMAP3 protein expression in knockdown animals.* Western blot analysis revealed a significant reduction of SLMAP3 protein expression in the adult heart of knockdown mice (45.81% ± 9.581%, $p<0.001$, $n=6$). Protein expression was analyzed via densitometry analysis by using α-Tubulin as a loading control. Copyright (2017) of Balwant Tuana laboratory at the University of Ottawa.

3.4 SLMAP1 and SLMAP2 protein levels were maintained in the SLMAP3 knockout hearts

While SLMAP3 protein was knocked out, the data shown in figure 10A indicates that anti-SLMAP recognized SLMAP1 and SLMAP2 protein in the SLMAP3 deficient hearts. Quantification of SLMAP1 (1.91% ± 31.94%, p=0.955, n=10) and SLMAP2 (12.86% ± 35.02%, p=0.74, n=10) bands were shown to have identical expression when compared to wildtype littermates (**Figure 10B**). This result indicates that targeting exon 3 of the SLMAP gene results in the knockout of SLMAP3 but not SLMAP1 or SLMAP 2 isoforms.

A.

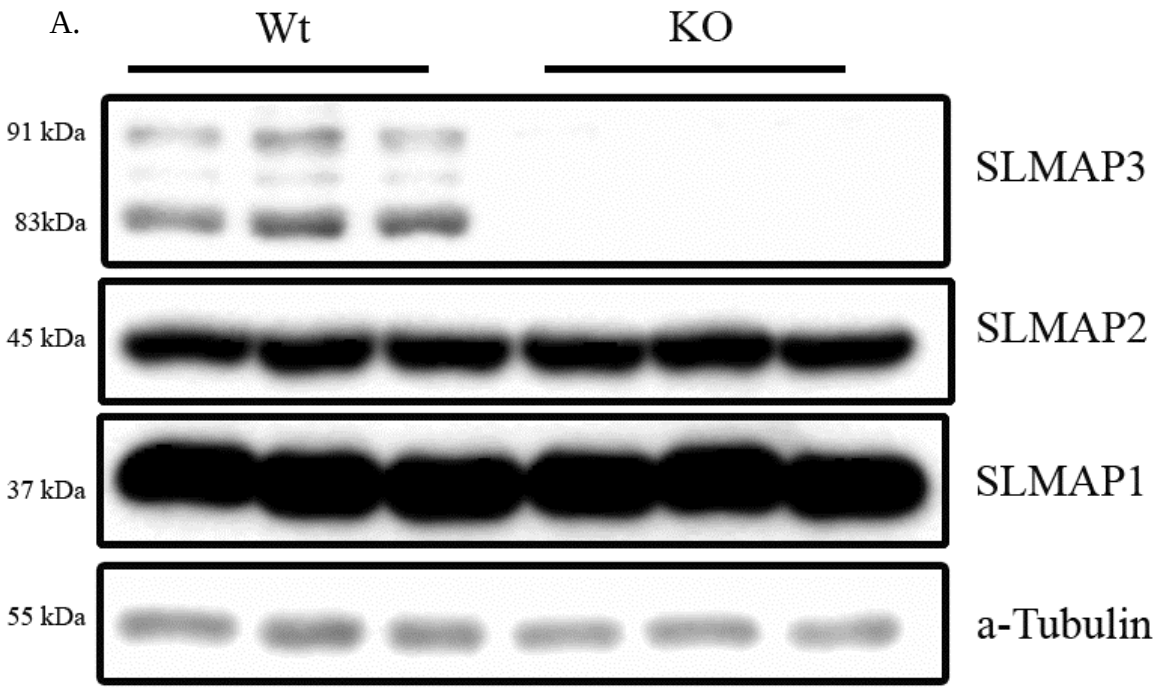
Wt
KO
91 kDa
83kDa
SLMAP3
45 kDa
SLMAP2
37 kDa
SLMAP1
55 kDa
a-Tubulin

B.

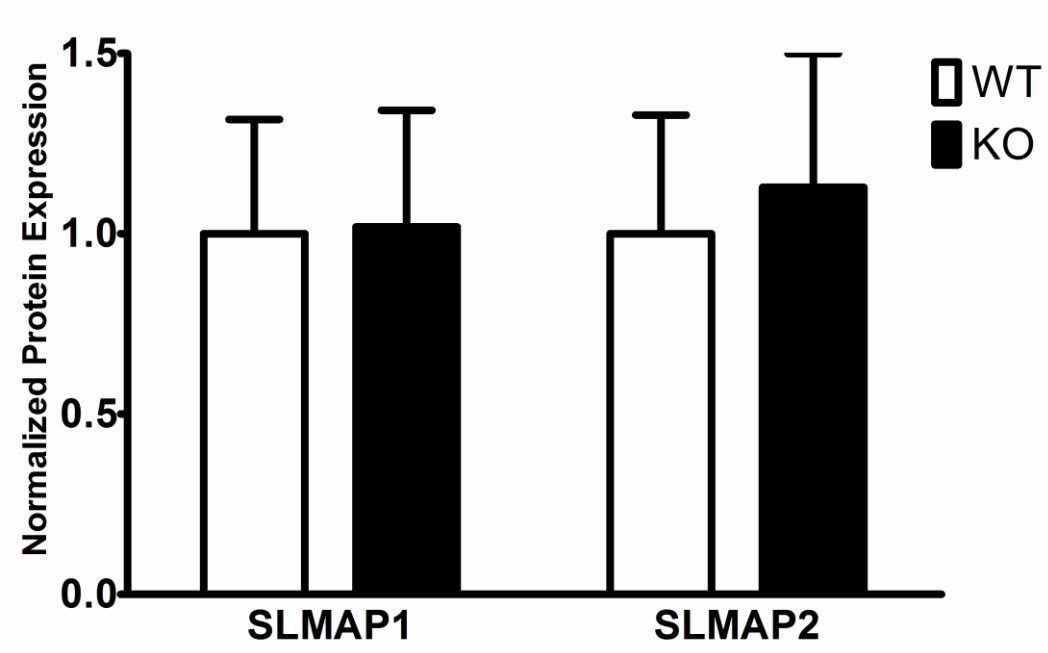
Normalized Protein Expression
1.5
1.0
0.5
0.0
WT
KO
SLMAP1
SLMAP2

Figure 10. *SLMAP isoform expression in knockout animals.* A) Western blot analysis was used to determine SLMAP expression in tamoxifen-treated knockout adult hearts. Anti-SLMAP did not detect any SLMAP3 protein in the knockout hearts (n=10). Anti-SLMAP detected SLMAP1 and SLMAP2 isoforms in wildtype and knockout hearts. B) Densitometry analysis using α-Tubulin as a loading control confirmed no significant changes in SLMAP1 (1.91% ± 31.94%, p=0.955, n=10) and SLMAP2 (12.86% ± 35.02%, p=0.74, n=10) in the KO hearts compared to WT. Copyright (2017) of Balwant Tuana laboratory at the University of Ottawa.

3.5 Transcript levels of SLMAP3 were specifically reduced in knockdown and knockout animals

I next examined the transcript levels of the three isoforms of SLMAP to determine if the changes in protein expression of SLMAP isoforms were reflective. To determine transcript levels of total SLMAP versus SLMAP3, specific primers were developed; SLPN-F/558-R and GTY-F/GTY-R. SLMAP gene contains exons at the 5' end, which are absent in SLMAP1 and SLMAP2 but expressed in SLMAP3 (Wigle, et al., 1997). I target the 5' region with primers SLPN-F/588-R which amplifies SLMAP3 only. Following this I observed a significant decrease in the KD (-55% ± 27%, n=19, $p<0.001$) and KO (-93.47% ± 31.2%, n=13, $p<0.001$) hearts transcript levels for SLMAP3 (**Figure 11A**).

SLMAP1 and SLMAP2 sequences are highly conserved in SLMAP3 therefore we are unable to specifically amplify these distinct isoforms individually. I use GTY-F/ GTY-R, a primer that targets all three isoforms to determine if there are any differences in total SLMAP mRNA expression post-tamoxifen. Total SLMAP expression in KD (-1.292% ± 38.35%, n=10, p=0.759) and KO (-34% ± 40.71%, n=9, p=0.759promoter) hearts revealed no significant differences in their respective transcript levels compared to wildtype (**Figure 11B**).

A.

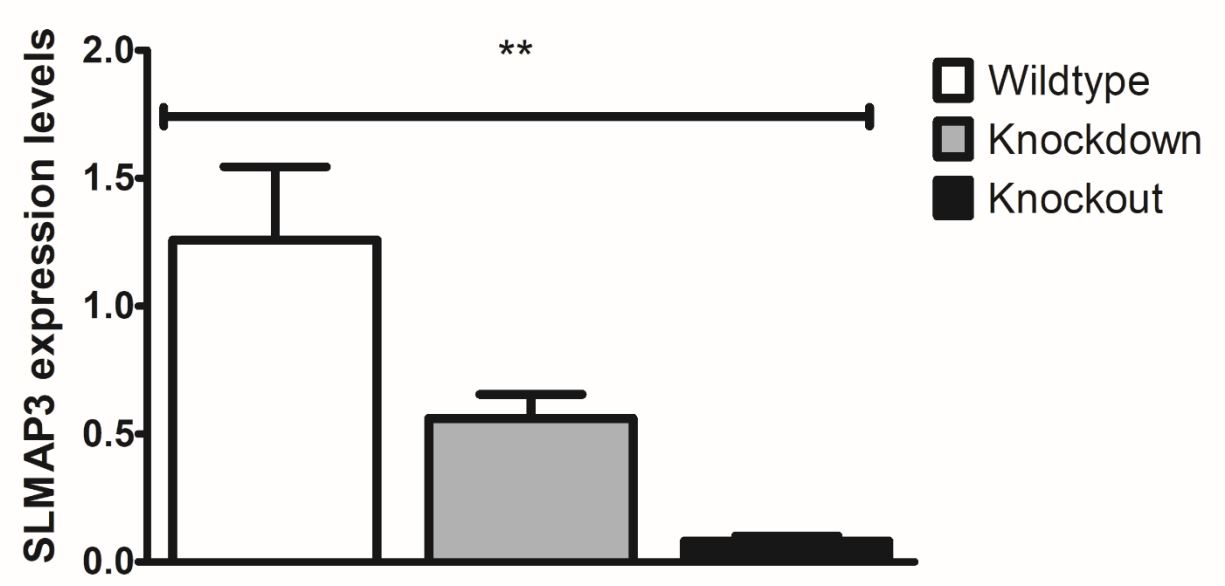
SLMAP3 expression levels
2.0
1.5
1.0
0.5
0.0
**
Wildtype
Knockdown
Knockout

B.

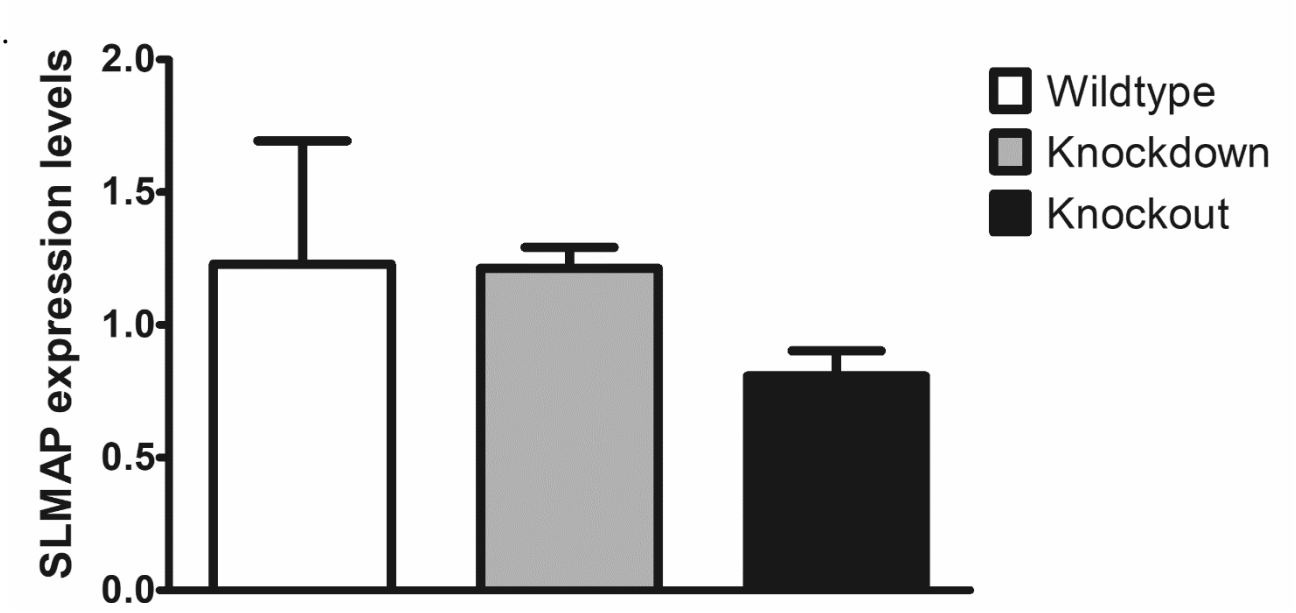
SLMAP expression levels
2.0
1.5
1.0
0.5
0.0
Wildtype
Knockdown
Knockout

Figure 11. *Transcript levels of SLMAP isoforms in knockout, knockdown and wildtype mice.* A) SLMAP3 cDNA fold change was determined using primers SLPN-F/588-R that revealed a reduction of SLMAP3 mRNA in both knockdown (-55%± 27%, n=19, $p<0.001$) and knockout (-93.47% ± 31.2%, n=13, $p<0.001$) mouse hearts. B) Total SLMAP cDNA fold change was analyzed using primers GTYF/GTYR, revealing no significant changes in KD (-1.292% ± 38.35%, n=10, $p=0.759$) and KO (-34% ± 40.71%, n=9, $p=0.759$) hearts when compared to Wt. Fold change was calculated using 18S-Ribosome as the normalizing control. P value was calculated using ANOVA statistics analysis.

3.6 Analysis of cardiac function in SLMAP3 deficient hearts

Cardiomyopathy is a heart disease which enlarges the LV causing hypertrophic cardiomyopathy (HCM) or dilated cardiomyopathy (DCM) (Marian & Roberts, 2001; Seidman & Seidman, 1998). As mentioned earlier, both cardiomyopathies were linked to mutations in the cardiac proteins localized to the sarcolemma of the cardiomyocyte (titin, β-MyHC) (Herman, et al., 2012). SLMAP is shown to be localized within the SR and the sarcolemma of the cardiomyocyte therefore I wanted to determine whether deficiency of SLMAP3 would result in any cardiac phenotypes i.e. cardiomyopathies.

Transthoracic echocardiography (ECHO) was used to assess any functional changes in tamoxifen treated animals. First set of ECHO images were recorded at 5-weeks post-tamoxifen (post-TAM) and followed for 18 weeks to observe any functional changes that include cardiac phenotypes in young (5-week post-TAM) and old (24-week post-TAM) SLMAP3 deficient animals. There were no notable structural differences observed in LV size or shape in the young or old SLMAP3 deficient mice when observed to the wildtype (**Figure 12A)**. Analysis of LV was done by measuring wall thickness; intraventricular septum (IVS), left ventricular posterior wall (LVPW) and left ventricular intradiameter (LVID) in both systole and diastole. Figure 12B highlights all the parameters that were measured in 5 week and 24-week post tamoxifen animals. The ejection fraction (EF) and fractional shortening (FS) is a useful parameter to determine cardiac health, as it is calculated by combining the aforementioned parameters. A cardiac phenotype results in lower EF% and FS% relative to wildtype (Yang, et al., 1999). The wall thickness in young and old SLMAP3 deficient mouse hearts were

not altered between the three groups therefore the EF% and FS% remained unchanged as well (**Figure 12B)**. The only observable difference noted was a slight increase in mass however that was most likely due to age-related cardiac growth. Therefore, a KD or KO of SLMAP3 results in no functional differences in the adult postnatal heart.

A.

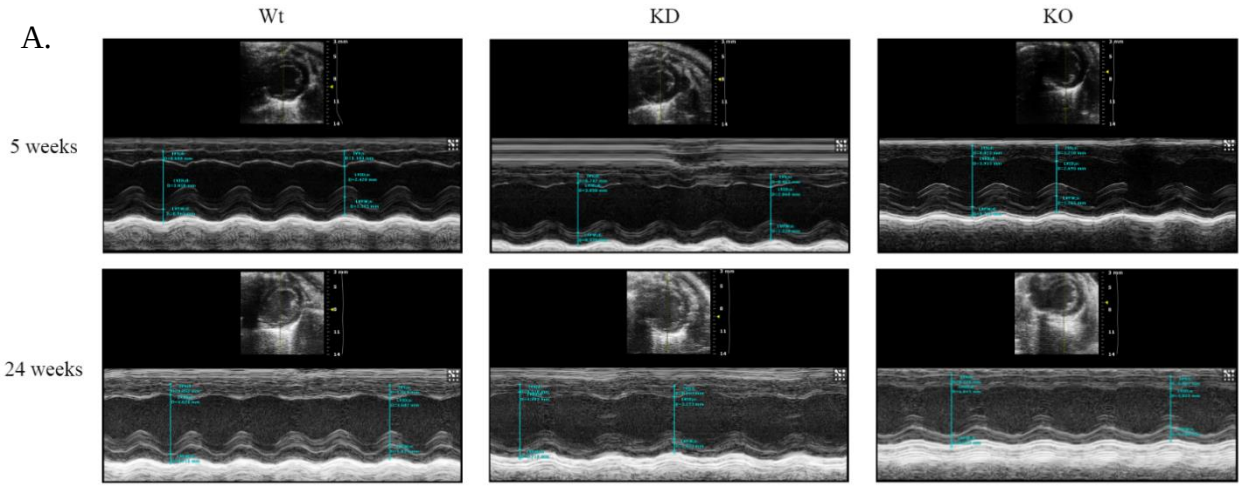

B.

5 week post TAM	WT	KD	KO	P<0.05
IVSd; mm	0.6764 ± 0.0346	0.7343 ± 0.0466	0.7213 ± 0.0387	N
IVSs; mm	0.9528 ± 0.06	1.0025 ± 0.0697	0.9334 ± 0.0661	N
LVIDd; mm	3.9965 ± 0.1029	3.8434 ± 0.087	3.9845 ± 0.0819	N
LVIDs; mm	2.9462 ± 0.1012	2.8760 ± 0.0794	2.9827 ± 0.1227	N
LVPWd; mm	0.7620 ±0.0463	0.8059 ± 0.0555	0.8107 ± 0.0677	N
LVPWs; mm	1.0144 ± 0.0619	1.0124 ± 0.0694	1.0246 ± 0.0767	N
EF; %	51.8357 ± 2.3254	50.3996 ± 1.3887	49.8972 ± 3.7079	N
FS; %	26.3304 ± 1.496	25.2116 ± 0.8434	25.2066 ± 2.2944	N
LV Mass; µg	102.6102 ± 6.9677	105.7861 ± 8.9723	110.9943 ± 9.140	N
LV Mass (Corrected); µg	82.0882 ± 5.5742	84.6289 ± 7.1779	88.7954 ± 7.3124	N
LV Vold; µL	70.5536 ± 4.2125	64.1029 ± 3.4144	69.6245 ± 3.3797	N
LV Vols; µL	34.1325 ± 2.7151	31.9205 ± 2.1479	35.0850 ± 3.5655	N

24 week post TAM	WT	KD	KO	P<0.05
IVSd; mm	0.7444 ± 0.01822	0.7289 ± 0.0236	0.7899 ± 0.0127	N
IVSs; mm	1.000 ± 0.0293	1.000 ± 0.0523	0.9957 ± 0.0810	N
LVIDd; mm	4.1938 ± 0.1208	4.1462 ± 0.0626	3.9812 ± 0.0415	N
LVIDs; mm	3.2809 ± 0.1161	3.1659 ± 0.0759	3.0276 ± 0.0512	N
LVPWd; mm	0.8699 ± 0.0389	0.76302 ± 0.0249	0.8596 ± 0.0489	N
LVPWs; mm	1.0739 ± 0.047	0.95973 ± 0.0407	1.0955 ± 0.0774	N
EF; %	44.6045 ± 1.2557	47.6106 ± 1.7636	48.0284 ± 3.7800	N
FS; %	21.8941 ± 0.6923	23.6991 ± 1.0618	23.8972 ± 2.2698	N
LV Mass; µg	129.9125 ± 8.0773	113.7697 ± 3.3335	121.6444 ± 5.9295	N
LV Mass (Corrected); µg	103.9300 ± 6.4618	91.0158 ± 2.6668	97.3155 ± 4.7439	N
LV Vold; µL	79.1529 ± 5.2612	76.4223 ± 2.6834	69.2567 ± 1.9777	N
LV Vols; µL	44.2800 ± 3.6378	40.1987 ± 2.1916	35.8462 ± 1.7474	N

Figure 12. *Echocardiography and left ventricular function in SLMAP3 knockdown and knockout mice.* A) Representative short axis m-mode images of wildtype, knockdown and knockout animals 5 weeks and 24 weeks post tamoxifen. B) Left ventricular functional analysis was done via measurements of wall sizes and intradiameter in diastole and systole. Measurements showed no significant changes in Wt, KD, or KO animals in both 5 weeks (P = 0.995) or 24 weeks (P = 0.986) post tamoxifen. P value was calculated using ANOVA statistics analysis. IVS; intraventricular septum, LVID; Left ventricular intradiameter, LVPW; Left ventricular posterior wall, EF; ejection fraction, FS; fractional shortening, LV mass; left ventricular mass, LV volume; left ventricular volume, d/s; diastole/systole. Copyright (2017) of Balwant Tuana laboratory at the University of Ottawa.

3.7 SLMAP3 deficient and wildtype mice had an identical response to isoproterenol

Our next aim was to administer isoproterenol (ISO) to SLMAP3 deficient mice to stress their hearts to evaluate their response to the stress and attempt to unmask a phenotype (Gramlich, et al., 2009). ISO delivery causes an increase in ventricle wall thickness subsequently resulting in pathological cardiac hypertrophy (Major, et al., 2015). Seven-day delivery of ISO (30ug/g) was mediated through mini-osmotic pumps that were subcutaneously implanted in eight-week-old adult mice that were genotyped KO or Wt. These animals were divided into two groups; each group would receive saline or ISO. Saline pump was used as a control for effects of pump implantation and changes that would naturally occur during the seven-day treatment. ECHOs were performed before pumps were implanted (preISO) and seven days after implantation (postISO). PostISO ECHOs revealed a significant change in wall thickness (**Figure 13A**). IVS;d postISO was significantly thicker ~0.7 mm to ~0.85 mm in KO and Wt hearts. LVPW;d postISO followed the same trend, from ~0.7 mm to ~0.9 mm in KO and Wt hearts. Unsurprisingly the weight of the hearts increased as a consequence of cardiac hypertrophy. Figure 13B highlights the similarity in hypertrophy between the two iso-treated groups as all the parameters (diastole and systole) went up by ~0.2 mm. This result suggested that hypertrophic response is similar between the SLMAP3 deficient and wildtype heart.

The Wt and KO hearts were extracted to visualize the differences in cardiac structure dosed with saline or ISO. Hearts were sectioned longitudinally and underwent histological staining via hematoxylin and eosin (H&E). H&E

stains the cardiomyocytes red thus we are able to visualize the myocardium size and length. Seven day ISO treatment resulted in no obvious differences between structure of KO or Wt hearts (**Figure 14).**

A.

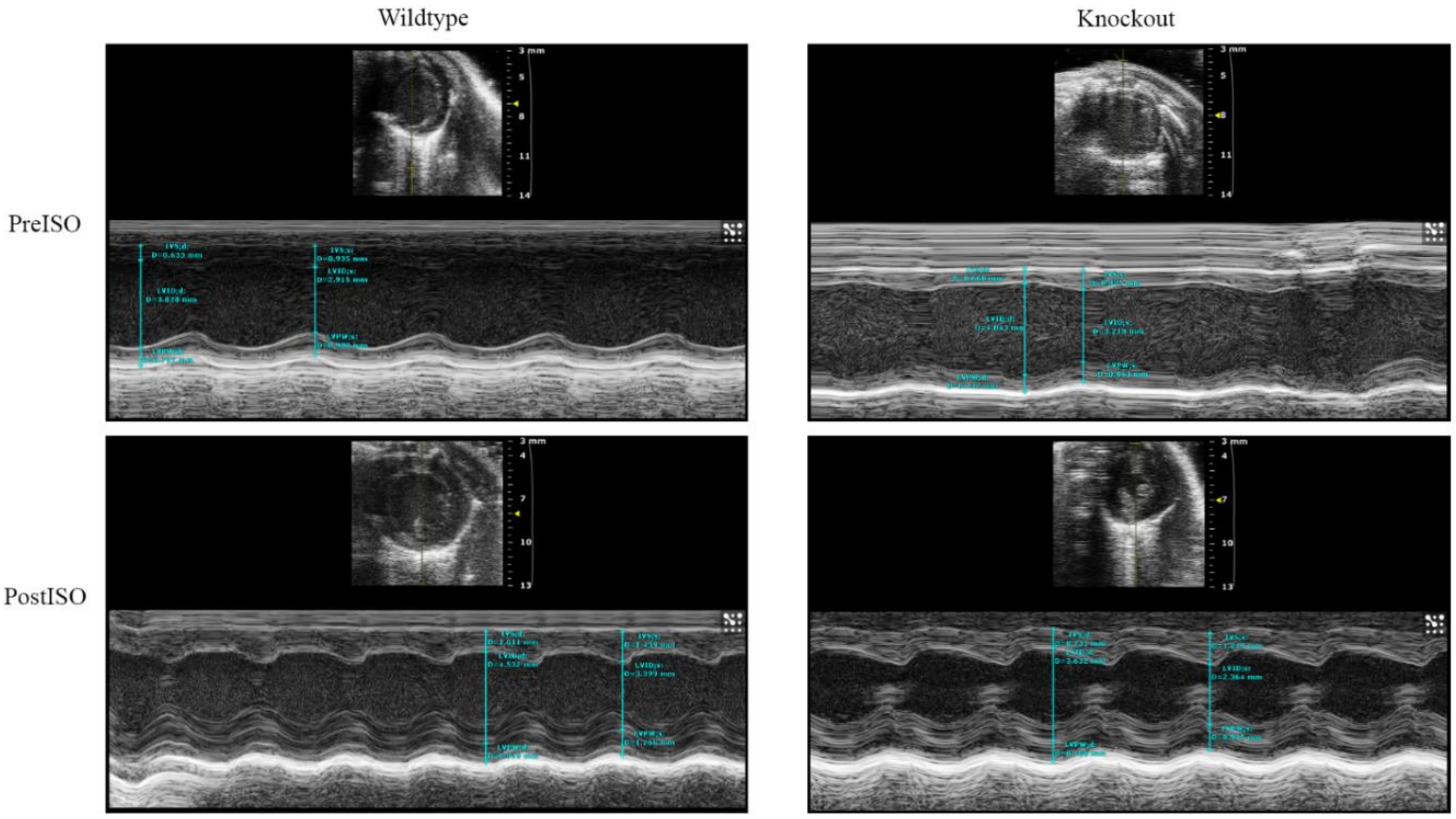

B.

Parameters	preISO WT	postISO WT	P value
IVSd; mm	0.687 ± 0.019	0.860 ± 0.030	0.000243881
IVSs; mm	0.964 ± 0.030	1.212 ± 0.048	0.001577668
LVPWd; mm	0.794 ± 0.031	0.917 ± 0.026	0.008476034
LVPWs; mm	1.044 ± 0.031	1.227 ± 0.035	0.002630256
LV Mass; µg	103.3 ± 4.175	139.0 ± 9.326	0.002448262
LV Mass (Corrected) ; µg	82.61 ± 3.756	111.2 ± 7.461	0.002448262

Parameters	preISO KO	postISO KO	P value
IVSd; mm	0.710 ± 0.0369	0.873 ± 0.0676	0.004832328
IVSs; mm	0.973 ± 0.0358	1.199 ± 0.084	0.029518316
LVPWd; mm	0.721 ± 0.0368	0.905 ± 0.038	0.010458202
LVPWs; mm	0.976 ± 0.0675	1.169 ± 0.038	0.014591292
LV Mass; µg	100.4 ± 5.932	127.2 ± 14.77	0.041526466
LV Mass (Corrected) ; µg	80.29 ± 4.746	101.74 ± 11.82	0.041526465

Figure 13. *Echocardiography and left ventricular function in ISO challenged KO and Wt mice.* A) Representative short axis m-mode images of wildtype and knockout animals preISO and postISO. B) Left ventricular functional analysis was done via measurements of wall sizes and intradiameter in diastole and systole. Significant changes in wall sizes were observed in WT and KO animals after ISO treatment. No changes were observed between the WT and KO postISO treatment. Copyright (2017) of Balwant Tuana laboratory at the University of Ottawa.

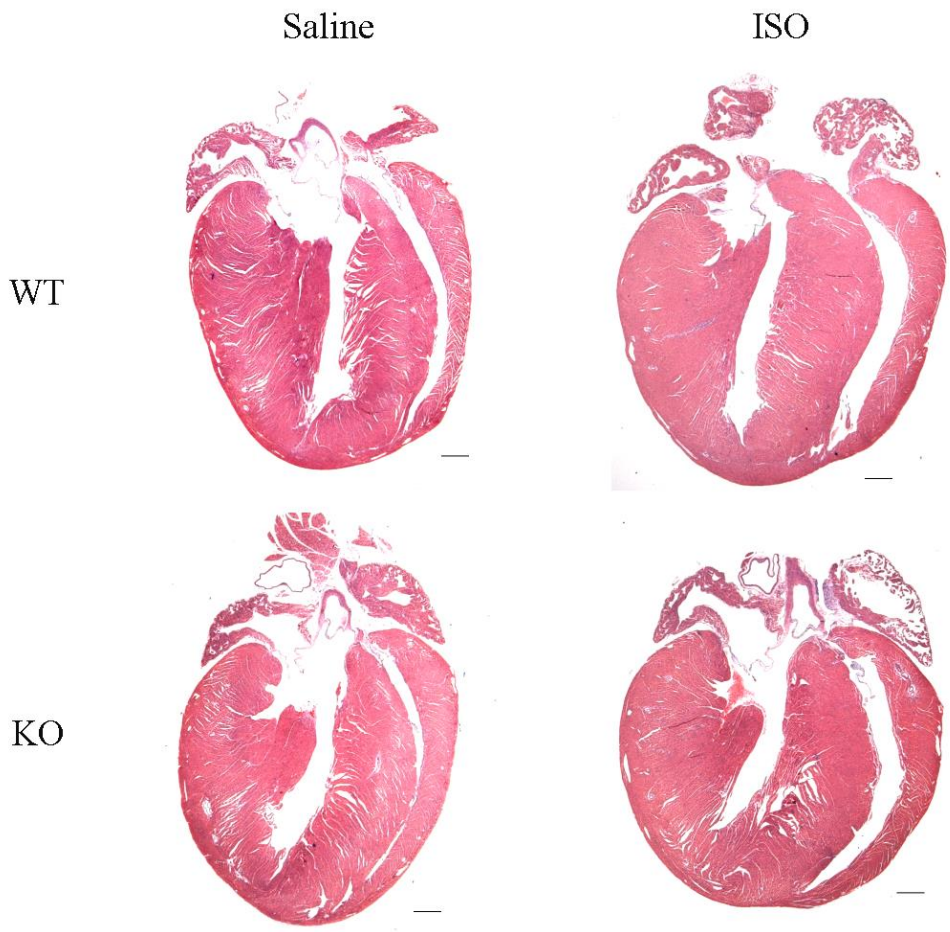

Figure 14. *Histological analysis of ISO challenged Wt and KO mouse hearts.* Representative sectioning of Wt or KO hearts after one week of saline or ISO were sectioned and stained with H&E to visualize the myocardium. Scale bar = 500 µm x 11.5 magnification. Copyright (2017) of Balwant Tuana laboratory at the University of Ottawa.

3.8 SLMAP3 deficient mice shows no changes to vesicle trafficking proteins

To explore impact of SLMAP3 deficiency on vesicle trafficking I examined the expression of proteins involved in intracellular trafficking. As discussed, previous studies have indicated that SLMAP regulate vesicle trafficking. This was observed firsthand in our aforementioned SLMAP1 overexpression transgenic (tg) mouse model which resulted in enlarged early endosomes that interacted with the endosomal recycling complex to upregulate GLTU4. To evaluate the impact of SLMAP3 KO in trafficking I examined the expression in SNARE proteins, EEA1 and Rabaptin-5. Thus, the SLMAP1-tg model was revisited to determine the expression and localization of proteins involved in the upregulation of vesicle trafficking which was then compared to SLMAP3 KO model.

The first parameter that I examined was early endosomal antigen 1 (EEA1), a tethering protein that facilitates the interaction of early endosomes to bind to each other (Christoforidis, et al., 1999). This proximity interaction or docking allows the SNARE proteins on the early endosomes to form a SNARE complex which initiates membrane fusion and forms a newly fused early endosome (Christoforidis, et al., 1999). SLMAP1-tg and Wt neonatal cardiomyocytes underwent immunofluorescent analysis via staining with EEA1 (magenta) and SLMAP (green) (**Figure 15**). SLMAP was used as a control marker to compare localization of EEA1 in the SLMAP1-tg cardiomyocytes relative to the wildtype. The wildtype cardiomyocyte displayed localization of EEA1 within early endosome vesicles (Pearson R-value 0.52 ± 0.063) however the transgenic hearts displayed an even greater localization and concentration of

EEA1 within the enlarged early endosomes (Pearson R-value 0.81 ± 0.029). The protein expression of EEA1 was also analyzed in tg hearts and was shown to be significantly upregulated in comparison to wildtype (168% ± 44.2%, n=4, $p<0.01$) (**Figure 16B)**. In the SLMAP3 KO model, EEA1 was shown to be maintained in the KO hearts (8.40% ± 26.60%, n=10, p=0.763) when compared to the wildtype (**Figure 17**). Expression of Rabaptin-5 was also analyzed as it plays an important role in early endosome fusion and was significantly upregulated in the SLMAP1-tg model. The expression of Rabaptin-5 (-18.9% ± -24.05%, n=10, p=0.460) in the SLMAP3 KO model, however, is unaffected.

Formation of a SNARE complex is critical for vesicle trafficking to take place, thus identifying SNARE proteins involved in early endosome fusion in SLMAP1-tg mice was imperative. Previous research has shown that SNARE proteins involved in early endosome fusion are SNAP23, SYN-4 and VAMP2 (Peters, et al., 2006). Based on this, I determined the localization and expression of these three SNARE proteins in the SLMAP1-tg hearts. Similar to EEA1, Wt and SLMAP1-tg cardiomyocytes underwent immunofluorescent analysis via staining with SNAP23, VAMP2, and SYN-4 (magenta) and SLMAP (green). The Wt cardiomyocytes display SLMAP and SNAREs signals to be evenly spread out throughout the cell (**Figure 16A**). In the SLMAP1-tg cardiomyocytes, SLMAP significantly co-localizes with SNAP23 (Pearson R-value 0.90 ± 0.02) and SYN-4 (Pearson R-value 0.91 ± 0.02) within the enlarged endosome. Interestingly, VAMP2 was not found inside the enlarged vesicles (Pearson R-value -0.20 ± 0.06) however we do see a concentration of VAMP2 surrounding the early

endosome suggesting that SLMAP1 is recruiting the VAMP2 v-SNARE towards the vesicles for SNARE driven membrane fusion. This theory was further enhanced when I examined the expression of SNARE proteins in the tg mouse hearts and noted a significant upregulation in SNAP23 (187% ± 60.3%, n=6, $p<0.05$), Syntaxin-4(133% ± 53.04%, n=4, $p<0.01$), and VAMP2 (96.13% ± 26.2%, n=5, $p<0.05$) in the transgenic mouse heart compared to wildtype (**Figure 16B**). When SNARE protein expression was analyzed in the SLMAP3 KO model, analysis indicated no significant changes in SNAP23 (-18.04% ± -27.76%, n=10, p=0.533), VAMP2 (-24.49% ± -38.88%, n=10, p=0.55) or Syntaxin-4 (-9.93% ± -31.56%, n=10, p=0.77) were found compared to the wildtype (**Figure 17**). Therefore, SLMAP3 KO has no effect on the endosomal recycling machinery that was impacted by the overexpression of SLMAP1 in the tg model.

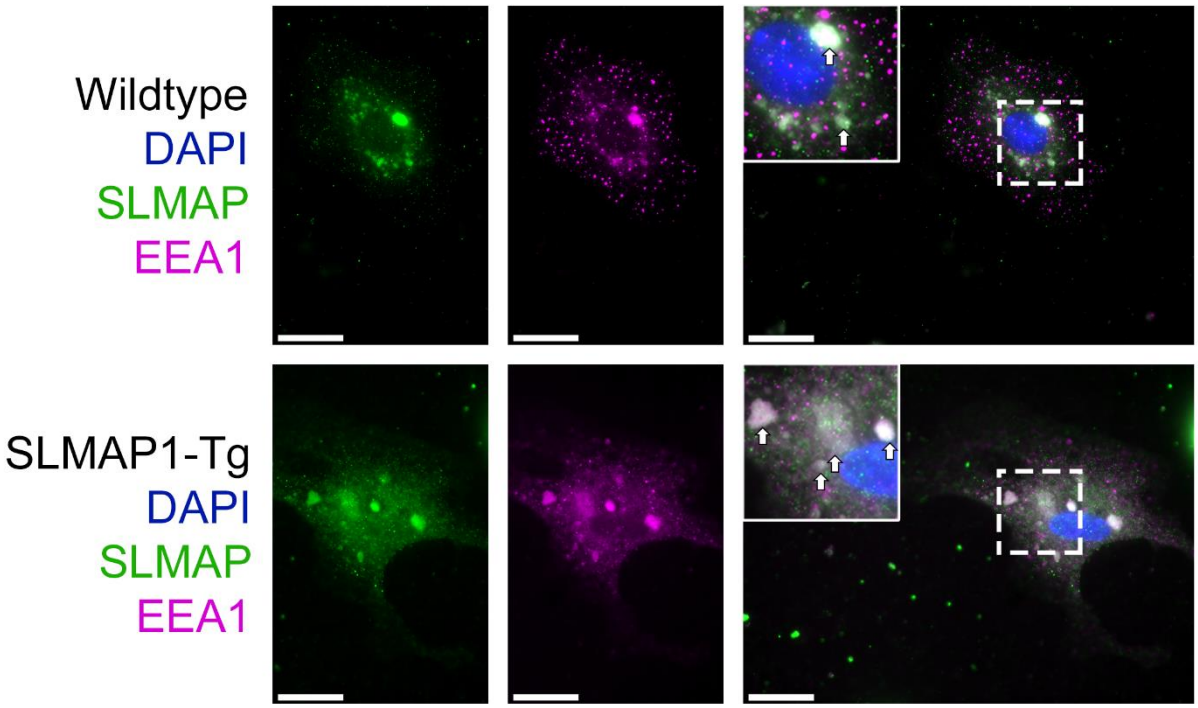

Figure 15. *Co-localization of SLMAP1 with EEA1.* Immunofluoresence co-staining of neonatal cardiomyocytes visualizing EEA1, total SLMAP, and SLMAP1 using anti-EEA1 (magenta), anti-SLMAP (green in wildtype), and anti-Myc (green in SLMAP1-Tg) antibodies respectively. Colocalization of EEA1 and SLMAP was observed in the wildtype cardiomyocytes. Greater colocalization of EEA1 and SLMAP1 was observed in the overexpressed SLMAP1 cardiomyocyte. White boxes represent zoomed regions and arrows denote regions of co-localization. Figure originally published in (Dewan, 2016) by permission from Taha Rehmani. Copyright (2017) of Balwant Tuana laboratory at the University of Ottawa.

A.

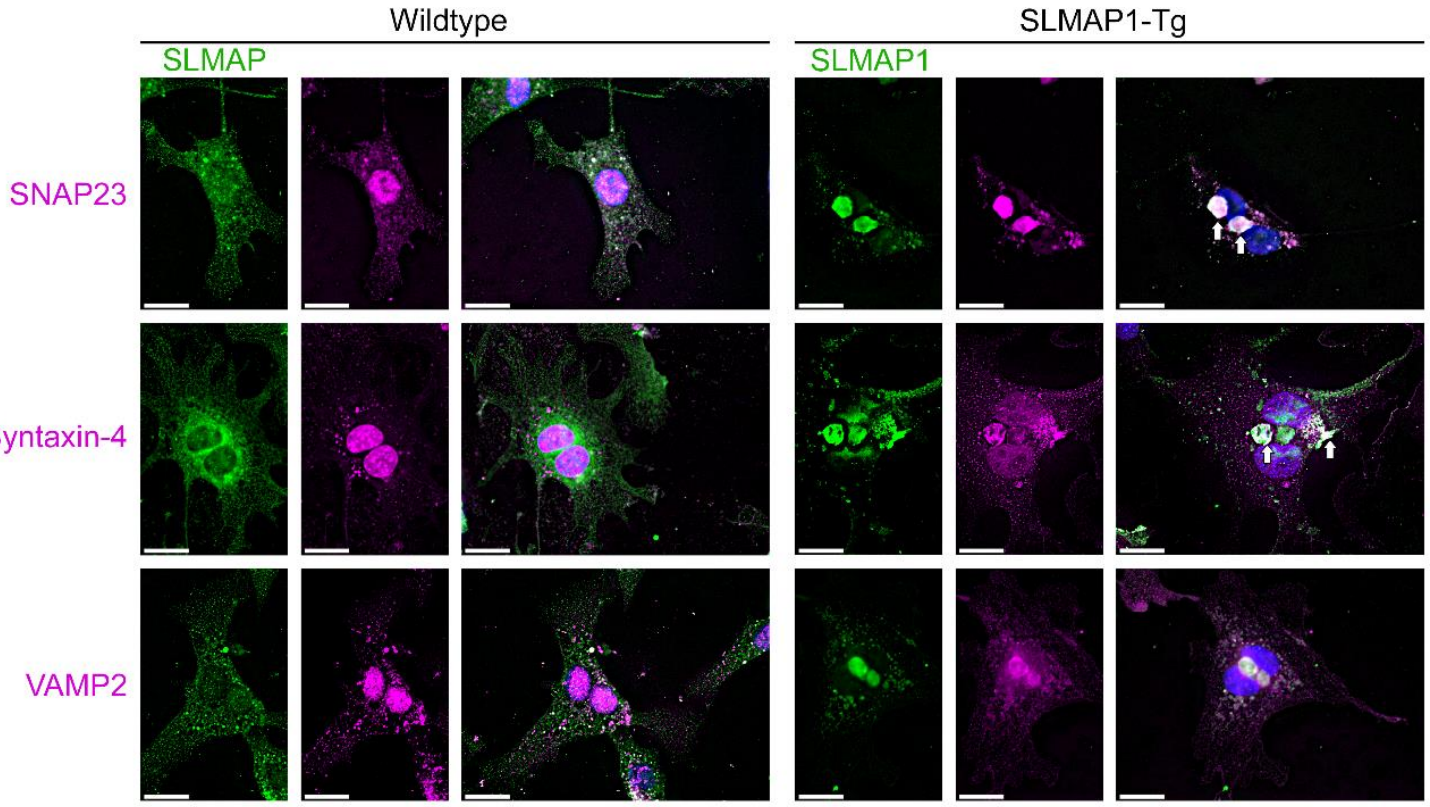
Wildtype
SLMAP1-Tg
SLMAP
SLMAP1
SNAP23
Syntaxin-4
VAMP2

B.

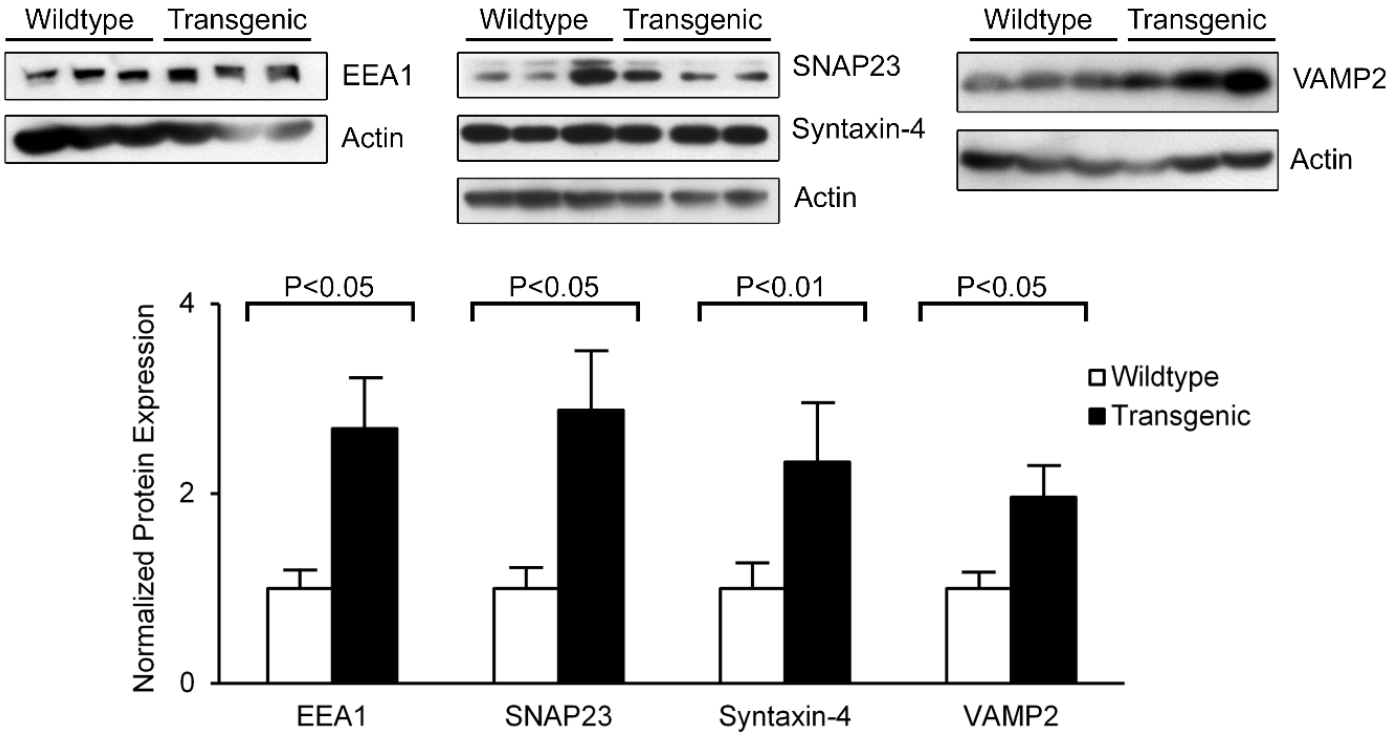
Wildtype
Transgenic
EEA1
Actin
SNAP23
Syntaxin-4
VAMP2
P<0.05
P<0.05
P<0.01
P<0.05
Normalized Protein Expression
4
2
0
Wildtype
Transgenic
EEA1
SNAP23
Syntaxin-4
VAMP2

Figure 16. *SLMAP1 overexpression recruits SNARE complex to form enlarged early endosomes.* (**A**) Neonatal cardiomyocytes visualizing SNARE proteins and SLMAP. SNAREs were visualized using anti-Syntaxin-4, anti-SNAP23, and anti-VAMP2 (magenta). Anti-SLMAP (green in wildtype) visualized SLMAP proteins in wildtype cardiomyocytes and anti-Myc (green in SLMAP1-Tg) visualized SLMAP1 in SLMAP1-Tg cardiomyocytes. Syntaxin-4 and SNAP23 showed significant colocalization with SLMAP1 (indicated by arrowheads) in the tg cardiomyocytes. VAMP2 was observed to be mutually exclusive, however VAMP2 was concentrated around the endosomes. (**B**) EEA1 and SNARE proteins were revealed to be upregulated in the transgenic mouse myocardium. EEA1 (168% ± 44.2%, n=4 adult hearts, $P<0.01$), SNAP23 (187% ± 60.3%, n=6 adult hearts, $P<0.05$), Syntaxin-4 (133% ± 53.04%, n=4 adult hearts, $P<0.01$) and, VAMP2 (96.13% ± 26.2%, n=5 adult hearts, $P<0.05$) was increased in transgenic hearts compared to wildtype hearts. Protein expression was assessed by western blot analysis and quantified using actin as a loading control. Figure originally published in (Dewan, 2016) by permission from Taha Rehmani. Copyright (2017) of Balwant Tuana laboratory at the University of Ottawa.

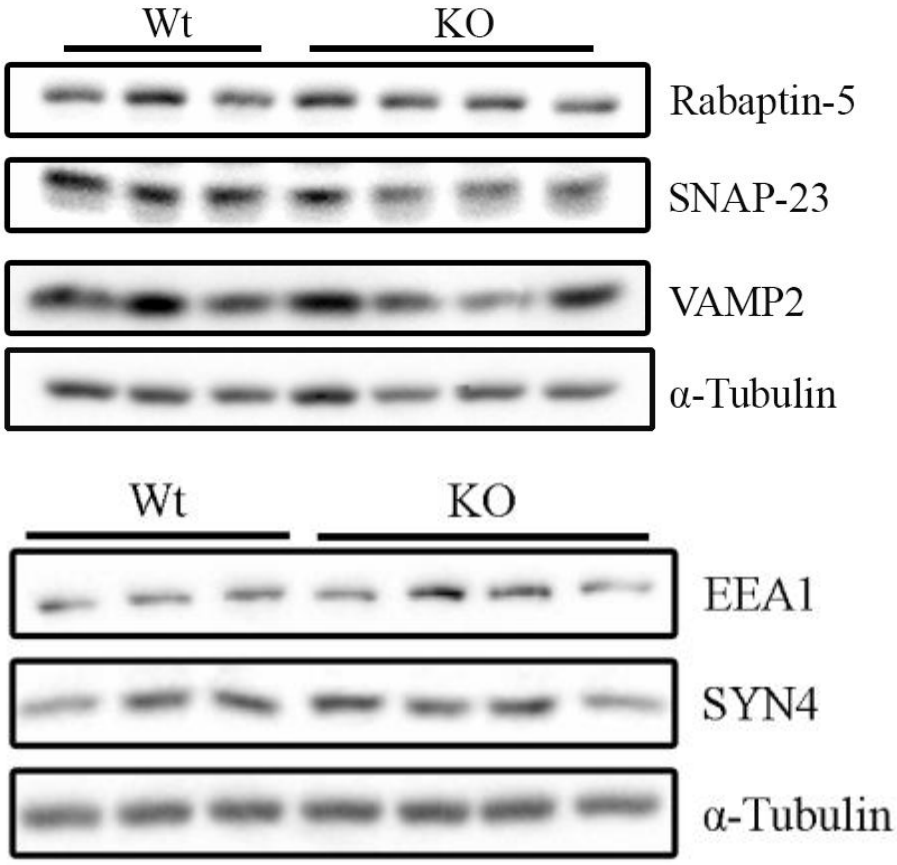
Wt
KO
Rabaptin-5
SNAP-23
VAMP2
α-Tubulin
Wt
KO
EEA1
SYN4
α-Tubulin

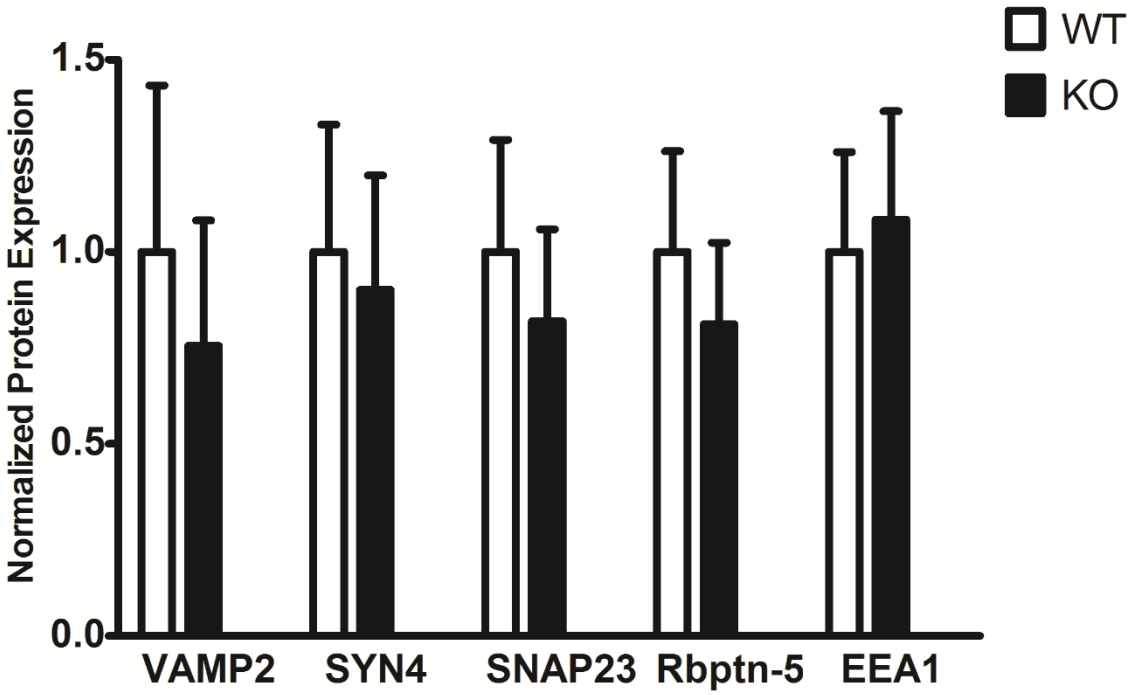
WT
KO
Normalized Protein Expression
1.5
1.0
0.5
0.0
VAMP2
SYN4
SNAP23
Rbptn-5
EEA1

Figure 17. *Endosomal protein expression of in knockout and wildtype animals.* Western blot analysis to determine expression of Rabaptin-5, EEA1 and SNARE proteins in knockout myocardium. Analysis indicated no changes in expression levels of SNAP23 (-18.04% ± -27.76%, n=10, p=0.533), VAMP2 (-24.49% ± -38.88%, n=10, p=0.55), Syntaxin-4 (-9.93% ± -31.56%, n=10, p=0.77), EEA1 (8.40% ± 26.60%, n=10, p=0.763) or Rabaptin-5, Rbtn-5, (-18.9% ± -24.05%, n=10, p=0.460) was observed in the KO hearts compared to the wildtypes. Protein expression was analyzed via densitometry analysis by using α-Tubulin as a loading control. Copyright (2017) of Balwant Tuana laboratory at the University of Ottawa.

Chapter 4: Discussion

The Cre-Lox model utilized in our study successfully knocked out SLMAP3 in the postnatal mouse myocardium. The α-MyHC-MerCreMer played a significant role, allowing us to control the "when" of the knockout via tamoxifen, and the "where" by expression of a cardiac specific promoter (Sohal, et al., 2001). This spatial and temporal knockout model for SLMAP was chosen because previous attempts at knocking out SLMAP using a promoter trap mutation resulted in prenatal lethality in a mouse model (Tuana, data not published). While the lethality was a significant phenotype, promoter trap mutation caused a global knockout therefore it would be difficult to evaluate the main cause of death. By using the α-MyHC-MerCreMer-Lox we could circumvent prenatal knockout of SLMAP and target the heart, thus directly evaluating the postnatal myocardium response to a deficiency of SLMAP.

While our initial aim was to establish a knockout of SLMAP in the postnatal myocardium I immediately observed that only SLMAP3 protein expression was being significantly altered in the KD or KO mice at both the protein and RNA levels. SLMAP1 and SLMAP2 expression was analyzed and no differences were observed when compared to the wildtype at the protein level. By using GTY-F/GTY-R I observed the total levels of SLMAP mRNA were preserved in the knockdown and knockout hearts. Since SLMAP1 and SLMAP2 transcripts are far in excess of SLMAP3 and as such no changes in total SLMAP was noted (discussed below). Therefore, the smaller isoforms remain unaffected by exon 3 cleavage in the postnatal heart. Therefore, by cleaving exon 3 of

SLMAP only results in the KD or KO of the largest isoform, SLMAP3. We theorize that SLMAP1 and SLMAP2 are not affected by this cleavage because they might be regulated by alternate promoters (TA & Van De Ven, 1996). GATA5 is a transcription factor that exhibits spatial and temporal patterns of expression, highly involved in mouse development and postnatal expression (Chen, et al., 2009). When a knockout of GATA5 took place in a mouse model, it was resulted in subtle phenotypes unlike the zebrafish model (Molkentin, et al., 2000). It was discovered that an alternate promoter region of the mouse GATA5 gene was initiating transcription in a novel start site found in intron 1. This truncated GATA5 was still functional and was compensating for the knockout of the larger GATA5 protein (Chen, et al., 2009). Similarly, SLMAP1 and SLMAP2 contain in-frame start codons at exon 10 and 16 and could be regulated by promoters upstream of these start codons (Wielowieyski, et al., 2000)

After confirming the SLMAP3 KO I evaluated if this specific isoform deficiency resulted in any cardiovascular functional changes using echocardiography. The SLMAP3 deficient animals showed no significant changes in LV structure or function in the acute or chronic knockdown or knockout of SLMAP. Similarly, by adding ISO to the KO animal I observed no change in the hypertrophic response. These results suggest that SLMAP3 does not play a role in this aspect of cardiac structure or function or that SLMAP1 and SLMAP2 may compensate. The lack of phenotype in the KO animal might be due to a genetic redundancy that overlaps the function of SLMAP3 in the animals. A study showed that when MyoD, a transcription factor highly involved in muscle

differentiation, was knocked out it resulted in mice that were viable, fertile and contained no morphological or physiological abnormalities, due to another transcription factor being significantly upregulated (Rudnicki, et al., 1992). Similarly, we postulate that SLMAP1 and SLMAP2 may be involved in this compensation due a significant homology between the three isoforms (Guzzo, et al., 2004). Protein and mRNA levels of SLMAP1 and SLMAP2 were unaffected in the knockout hearts but because their level of expression in the myocardium is so high, it is believed they could still compensate for SLMAP3 in the knockout myocardium.

I then wanted to detect if SLMAP3 deficiency resulted in any changes to the intracellular trafficking pathway. In the SLMAP1-tg mouse model we observed enlarged vesicles that were discovered to be early endosomes due to localization of early endosome marker Rab5 within those vesicles (Dewan, 2016). We also saw a significant non-transcriptional upregulation of GLUT4 on the plasma membrane. Thus, we believed that GLUT4 was being upregulated by a recycling mechanism involving the enlarged early endosomes (Dewan, 2016). I observed a significant upregulation of EEA1, SNAP23, SYN-4, and VAMP2 and showed significant localization within the enlarged early endosome. The increase in EEA1 signifies an increase in docking between early endosomes and the increase in SNARE proteins results in more SNARE complexes being formed. Taken together these results suggest a model for enhancing early endosome fusion which can result in the enlarged early endosomes and vesicle trafficking in the SLMAP1-tg ultimately upregulating GLUT4 in the myocardium. When protein

expression levels of EEA1, Rabaptin-5, SNAP23, SYN-4, and VAMP2 were examined in the SLMAP3 KO model I observed no significant changes compared to wildtype. This result was unsurprising as the overexpression of the smallest SLMAP isoform. SLMAP1, caused enlargement of early endosomes and upregulation of the fusion machinery. Indeed, in our SLMAP3 overexpression model, myocardium was analyzed for these proteins and no differences were observed similar to our SLMAP3 KO model (data not shown).

SLMAP3 deficiency results in no significant changes to cardiovascular function or to intracellular trafficking in the postnatal myocardium. However, this SLMAP3 KO model can still be utilized in different settings to further our understanding about SLMAPs role in mammalian biology. There is sufficient evidence to show that SLMAP is developmentally regulated (Guzzo, et al., 2005). By causing a SLMAP3 KO in the mouse embryos we can determine SLMAP3 role in the developing heart. This can be facilitated by breeding flox-SLMAP animals with a Nkx2.5-Cre animal, a cardiac promoter that is expressed mainly within a developing heart (Moses, et al., 2001). Research done in our lab has implicated the 80 kDa SLMAP3 variant as a mediator for myoblast fusion (Guzzo, et al., 2004). Therefore, by using a muscle specific cre (MyoD-Cre) we can determine the effect a SLMAP3 KO would have on skeletal muscle and muscle formation (Chen, et al., 2005). Our lab has another transgenic mouse model which postnatally overexpresses cardiac-specific SLMAP3. This model has shown to be resistant to myocardial injury namely myocardial infarction, by surviving and outliving their wildtype littermates (Lefnaier, 2017). Therefore, it

would be a captivating study to determine how the SLMAP3 KO model responds to a similar type of myocardial injury such as an infarction or a transverse aortic constriction.

Finally, we must generate a model which results in the knockout of all three isoforms of SLMAP. We must target an area in the SLMAP gene that allows us to successfully knockout all three isoforms to enhance our understanding of SLMAPs role in the myocardium and intracellular trafficking. We can attempt to target another exon with loxP sites closer to the start sequences of SLMAP1 or SLMAP2 such as exon 16. Another method to generate a knockout is the use of CRISPR/Cas9 system (Sander & Joung, 2014). Many studies are being done to mediate a cardiac specific knockout by expressing Cas9 specifically within the heart and using an adeno-associated virus vector to deliver the 20bp single strand guide RNA (sgRNA) to the heart (Xie, et al., 2016). By designing multiple strands of sgRNA to target the SLMAP gene, this system could be utilized to knockout of SLMAP.

In conclusion, the knockdown or knockout of SLMAP3 in the postnatal myocardium has been achieved and does not appear to impact myocardium structure or function or expression of proteins involved in intracellular trafficking. My data indicates distinct isoform specific function and function of SLMAP3 might be compensated for in SLMAP1 and SLMAP2.

Chapter 5: References

Aken, B., Ayling, S., Barrell, D. & al, e., 2016. The Ensembl gene annotation system. *Database ,* Volume baw093, p. Release 90.

Amin, S. A., Hanno, T. & Wilde, A., 2010. Cardiac ion channels in health and disease. *Heart Rhythm,* 7(1), pp. 117-126.

Andersson, K. et al., 2010. Tamoxifen administration routes and dosage for inducible Cre-mediated gene disruption in mouse hearts. *Transgenic Res,* 19(4), pp. 715-25.

Austin, S., Ziese, M. & Sternberg, N., 1981. A novel role for site-specific recombination in maintenance of bacterial replicons.. *Cell,* Volume 25 , pp. 729-36.

Ayadi, A., Ferrand, G., Cruz, I. & Warot, X., 2011. Mouse Breeding and Colony Management.. *Current Protocols in Mouse Biology,* Volume 1, pp. 239-264.

Balse, E. et al., 2012. Dynamic of ion channel expression at the plasma membrane of cardiomyocytes. *Physiol Review,* 92(3), pp. 1317-58.

Bergmann, O. et al., 2009. Evidence for Cardiomyocyte Renewal in humans. *Science,* 324(5923), pp. 98-102.

Bersell, K. et al., 2013. Moderate and high amounts of tamoxifen in αMHC-MerCreMer mice induce a DNA damage response, leading to heart failure and death. *Disease Models & Mechanisms,* 6(6), pp. 1459-69.

Bett, G. et al., 2012. A Mouse Model of Timothy Syndrome: a Complex Autistic Disorder Resulting from a Point Mutation in Cav1.2.. *North American journal of medicine & science,* 5(3), pp. 135-140.

Bonifacino, J. & Glick, B., 2004. The mechanisms of vesicle budding and fusion. *Cell,* 116(2), pp. 153-66.

Bonini, N. & Giasson, B., 2005. Snaring the function of alpha-synuclein. *Cell,* 123(3), pp. 359-61.

Boudina, S. & Abel, E., 2010. Diabetic cardiomyopathy, causes and effects. *Reviews in endocrine & metabolic disorders,* 11(1), pp. 31-39.

Branda, C. & Dymecki, S., 2004. Talking about a revolution: The impact of site-specific recombinases on genetic analyses in mice. *Dev Cell,* 6(1), pp. 7-28.

Brandizzi, F. & Barlowe, C., 2014. Organization of the ER–Golgi interface for membrane traffic control. *Nat Rev Mol Cell Biol,* 14(6), pp. 382-392.

Brewer, P. et al., 2014. Insulin-regulated Glut4 translocation: membrane protein trafficking with six distinctive steps. *J Biol Chem,* 289(25), pp. 17280-98.

Brugada, R. et al., 2014. Brugada syndrome. *Methodist Debakey Cardiovasc J,* 10(1), pp. 25-8.

Buerger, A. et al., 2006. Dilated cardiomyopathy resulting from high-level myocardial expression of Cre-recombinase. *J Card Fail,* 12(5), pp. 392-8.

Burchfield, J., Xie, M. & Hill, J., 2013. Pathological Ventricular Mechanisms. *Circulation,* 128(4), pp. 388-400.

Bustin, S. A., 2002. Quantification of mRNA using real-time reverse transcription PCR (RT-PCR): trends and problems. *J Mol Endocrinol,* 29(1), pp. 23-29.

Byers, J., Guzzo, R., Salih, M. & Tuana, B., 2009. Hydrophobic profiles of the tail anchors in SLMAP dictate subcellular targeting. *BMC Cell Biol,* 10(48).

Cai, H., Reinisch, K. & Ferro-Novick, S., 2007. Coats, tethers, Rabs, and SNAREs work together to mediate the intracellular destination of a transport vesicle. *Developmental Cell,* 5(12), pp. 671-82.

Carrier, L. et al., 1997. Organization and sequence of human cardiac myosin binding protein C gene (MYBPC3) and identification of mutations predicted to produce truncated proteins in familial hypertrophic cardiomyopathy. *Circ Res,* 80(3), pp. 427-34.

Chen, B., Yates, E., Huang, Y. & al, e., 2009. Alternative promoter and GATA5 transcripts in mouse.. *American Journal of Physiology - Gastrointestinal and Liver Physiology,* 297(6), pp. 1214-1222.

Chen, J., Mortimer, J., Marley, J. & Goldhamer, D., 2005. MyoD-cre transgenic mice: a model for conditional mutagenesis and lineage tracing of skeletal muscle. *Genesis,* 41(3), pp. 116-21.

Chen, X. & Ding, H., 2011. Increased expression of the tail-anchored membrane protein SLMAP in adipose tissue from type 2 Tally Ho diabetic mice. *Exp Diabetes Res.*

Christoforidis, S., McBride, H., Burgoyne, R. & Zerial, M., 1999. The Rab5 effector EEA1 is a core component of endosome docking.. *Nature,* 397(6720), pp. 621-5.

Davis, J., Maillet, M., Miano, J. & Molkentin, J., 2012. Lost in transgenesis: a user's guide for genetically manipulating the mouse in cardiac research. *Circ Res,* 111(6), pp. 761-77.

Deneka, M., Neeft, M. & Popa, I., 2003. Rabaptin-5α/rabaptin-4 serves as a linker between rab4 and γ1-adaptin in membrane recycling from endosomes. *The EMBO Journal,* 22(11), pp. 2645-2657.

Dewan, A., 2016. *A Unique Role for Sarcolemmal Membrane Associated Protein Isoform 1 (SLMAP1) as a Regulator of Cardiac Metabolism and Endosomal Recycling.* [Online]
Available at: http://dx.doi.org/10.20381/ruor-843
[Accessed 19 August 2016].

Foley, K., Boguslavsky, S. & Klip, A., 2011. Endocytosis, recycling and regulated exocytosis of glucose transporter 4. *Biochemistry,* 50(15), pp. 3048-3061.

Fukuta, H. & Little, W., 2008. The cardiac cycle and the physiologic basis of left ventricular contraction, ejection, relaxation, and filling. *Heart Fail Clin,* 4(1), pp. 1-11.

Gagniuc, P. & Ionescu-Tirgoviste, C., 2012. Eukaryotic genomes may exhibit up to 10 generic classes of gene promoters. *BMC Genomics,* 13(512).

Gentzsch, M. et al., 2004. Endocytic trafficking routes of wild type and DeltaF508 cystic fibrosis transmembrane conductance regulator. *Mol Biol Cell,* 15(6), pp. 2684-96.

Gimeno, R. et al., 2003. Characterization of a heart-specific fatty acid transport protein. *J Biol Chem,* 278(18), pp. 16039-44.

Gonzalo, S., Greentree, W. & Linder, M., 1999. SNAP-25 is targeted to the plasma membrane through a novel membrane-binding domain. *J Biol Chem,* 274(30), pp. 21313-8.

Gramlich, M. et al., 2009. Stress-induced dilated cardiomyopathy in a knock-in mouse model mimicking human titin-based disease. *J Mol Cell Cardiol,* 47(3), pp. 352-8.

Grant, B. & Donaldson, J., 2009. Pathways and mechanisms of endocytic recycling. *Nat Rev Mol Cell Biol,* 10(9), pp. 597-608.

Grégoire, D. & Kmita, M., 2008. Recombination between inverted loxP sites is cytotoxic for proliferating cells and provides a simple tool for conditional cell ablation. *Proc Natl Acad Sci U S A,* 105(38), pp. 14492-6.

Guo, F., Gopaul, D. & van Duyne, G., 1997. Structure of Cre recombinase complexed with DNA in a site-specific recombination synapse. *Nature,* 389(6645), pp. 40-6.

Guzzo, R. M., Salih, M., Moore, E. D. & Tuana, B. S., 2005. Molecular properties of cardiac tail-anchored membrane protein SLMAP are consistent with structural role in arrangement of excitation-contraction coupling apparatus.. *Am J Physiol Heart Circ Physiol,* 288(4), pp. H1810-9.

Guzzo, R., Sevinc, S., M, S. & Tuana, B., 2004. A novel isoform of sarcolemmal membrane-associated protein (SLMAP) is a component of the microtubule organizing centre. *J Cell Sci,* 117(11), pp. 2271-81.

Guzzo, R. et al., 2004. Regulated expression and temporal induction of the tail-anchored sarcolemmal-membrane-associated protein is critical for myoblast fusion. *Biochem J,* 381(3), pp. 599-608.

Guzzo, R. et al., 2004. Regulated expression and temporal induction of the tail-anchored sarcolemmal-membrane-associated protein is critical for myoblast fusion. *Biochem J. 2004 Aug 1;381(Pt 3):599-608.,* 381(3), pp. 599-608.

Hall, J., 2011. *Guyton and Hall textbook of medical physiology.* Philedelphia: Saunders/Elsevie.

Hall, M., G, S., Hall, J. & Stec, D., 2011. Systolic dysfunction in cardiac-specific ligand-inducible MerCreMer transgenic mice. *Am J Physiol Heart Circ Physiol,* 301(1), pp. 253-60.

Hamilton, D. L. & Abremski, K., 1984. Site specific recombination oby the bacteriophage p1 lox-Cre system. *J. Mol. Biol,* Volume 178, pp. 481-486.

Harkcom, W. T. & Abbott, G., 2010. Emerging concepts in the pharmacogenomics of arrhythmias: ion channel trafficking. *Expert Rev Cardiovasc Ther,* 8(8), pp. 1161-73.

Hensley, N. et al., 2015. Hypertrophic cardiomyopathy: a review. *Anesth Analg,* 120(3), pp. 554-69.

Herman, D., Lam, L. & Taylor, M., 2012. Truncations of Titin Causing Dilated Cardiomyopathy. *The New England journal of medicine,* 366(7), pp. 619-628.

Heusch, G. & Schulz, R., 1996. Hibernating myocardium: a review. *J Mol Cell Cardiol,* 28(12), pp. 2359-72.

Hochman, L., Segev, N., Sternberg, N. & Cohen, G., 1983. Site-specific recombinational circularization of bacteriophage P1 DNA. *Virology,* 131(1), pp. 11-17.

Hoess, R., Wierzbicki, A. & Abremski, K., 1986. The role of the loxP spacer region in P1 site-specific recombination. *Nucleic Acids Res,* 14(1986), pp. 2287-2300.

Hong, W., 2005. SNAREs and traffic. *Biochim Biophys Acta,* 1744(2), pp. 120-44.

Hong, W. & Lev, S., 2014. Tethering the assembly of SNARE complexes. *Trends Cell Biol,* 24(1), pp. 35-43.

How, O. et al., 2006. Increased myocardial oxygen consumption reduces cardiac efficiency in diabetic mice. *Diabetes,* 55(2), pp. 466-473.

Hu, C. et al., 2003. Fusion of cells by flipped SNAREs. *Science,* 300(5626), pp. 1745-9.

Hu, D., Barajas-Martinez, H., Burashnikov, E. & al, e., 2009. A Mutation in the β3 Subunit of the Cardiac Sodium Channel Associated with Brugada ECG Phenotype. *Circulation Cardiovascular genetics,* 2(3), pp. 270-278.

Hunn, B. et al., 2015. Impaired intracellular trafficking defines early Parkinson's disease. *Trends in Neurosciences,* 38(3), pp. 178-188.

Ibrahim, M., Gorelik, J., Yacoub, M. & Terracciano, C., 2011. The structure and function of cardiac t-tubules in health and disease. *Proceedings of the Royal Society B: Biological Sciences,* 278(1719), pp. 2714-2723.

Ishikawa, T. et al., 2012. A novel disease gene for Brugada syndrome: sarcolemmal membrane-associated protein gene mutations impair intracellular trafficking of hNav1.5. *Circ Arrhythm Electrophysiol,* 5(6), pp. 1098-107.

Jahn, R. & Südhof, T., 1999. Membrane fusion and exocytosis. *Annu Rev Biochem,* 1999(68), pp. 863-911.

Jones, W., Sánchez, A. & Robbins, J., 1994. Murine pulmonary myocardium: developmental analysis of cardiac gene expression.. *Dev Dyn,* 200(2), pp. 117-28.

Kiermayer, C. et al., 2007. Optimization of spatiotemporal gene inactivation in mouse heart by oral application of tamoxifen citrate. *Genesis,* 45(1), pp. 11-6.

Kleber, A. & Saffitz, J., 2014. Role of the intercalated disc in cardiac propagation and arrhythmogenesis. *Frontiers in Physiology,* 5(404).

Koitabashi, N. et al., 2009. Avoidance of transient cardiomyopathy in cardiomyocyte-targeted tamoxifen-induced MerCreMer gene deletion models. *Circ Res,* 105(1), pp. 12-5.

Kouranti, I. et al., 2006. Rab35 regulates an endocytic recycling pathway essential for the terminal steps of cytokinesis. *Curr Biol,* 16(17), pp. 1719-25.

Kuhn, R. & Torres, R. M., 2002. Cre/LoxP Recombination System and Gene Targeting. *Transgenesis Techniques,* 180(V), pp. 175-204.

Lefnaier, W., 2017. *Potential Role for the Sarcolemmal Membrane Associated Protein Isoform 3 (SLMAP3) in Cardiac Remodeling Post Myocardial Infarction.* [Online]
Available at: http://hdl.handle.net/10393/35713
[Accessed 01 01 2017].

Littlewood, T. et al., 1995. A modified oestrogen receptor ligand-binding domain as an improved switch for the regulation of heterologous proteins. *Nucleic Acids Res,* 23(10), pp. 1686-1690.

Luk, A., Ahn, E., Soor, G. & Butany, J., 2009. Dilated cardiomyopathy: a review. *J Clin Pathol,* 62(3), pp. 219-25.

Mahmoud, A., Canseco, D., Xiao, F. & Sadek, H., 2014. Cardiomyocyte cell cycle: Meis-ing something?. *Cell Cycle,* 13(7), pp. 1057-1058.

Major, J., Salih, M. & Tuana, B., 2015. Interplay between the E2F pathway and β-adrenergic signaling in the pathological hypertrophic response of myocardium. *J Mol Cell Cardiol,* Issue 84, pp. 179-90.

Marian, A. & Roberts, R., 2001. The Molecular Genetic Basis for Hypertrophic Cardiomyopathy. *Journal of molecular and cellular cardiology,* 33(4), pp. 655-670.

Maxfield, F. & McGraw, T., 2004. Endocytic recycling. *Nat Rev Mol Cell Biol.,* 5(2), pp. 121-32.

McNally, E., Golbus, J. & Puckelwartz, M., 2013. Genetic mutations and mechanisms in dilated cardiomyopathy. *The Journal of Clinical Investigation,* 123(1), pp. 19-26.

Metzger, D., Clifford, J., Chiba, H. & Chambon, P., 1995. Conditional site-specific recombination in mammalian cells using a ligand-dependent chimeric Cre

recombinase. *Proceedings of the National Academy of Sciences of the United States of America,* 92(15), pp. 6991-6995.

Missirlis, P., Smailus, D. & Holt, R., 2006. A high-throughput screen identifying sequence and promiscuity characteristics of the loxP spacer region in Cre-mediated recombination. *BMC Genomics,* 7(73).

Molkentin, J., Tymitz, K., Richardson, J. & Olson, E., 2000. Abnormalities of the genitourinary tract in female mice lacking GATA5.. *Mol Cell Biol,* 20(14), pp. 5256-60.

Moses, K. et al., 2001. Embryonic expression of an Nkx2-5/Cre gene using ROSA26 reporter mice. *Genesis,* 31(4), pp. 176-80.

Mueckler, M., 2001. Insulin resistance and the disruption of Glut4 trafficking in skeletal muscle. *J Clin Invest,* 107(10), pp. 1211-1213.

Nader, M. et al., 2012. Tail-anchored membrane protein SLMAP is a novel regulator of cardiac function at the sarcoplasmic reticulum. *Am J Physiol Heart Circ Physiol,* 302(5), pp. 1138-1145.

Nerbonne, J. & Kass, R., 2005. Molecular physiology of cardiac repolarization. *Physiol Rev,* 85(4), pp. 1205-53.

Orban, P., D, C. & Marth, J., 1992. Tissue- and site-specific DNA recombination in transgenic mice. *Proceedings of the National Academy of Sciences of the United States of America.,* 89(15), pp. 6861-6865.

Pasqualini, F. et al., 2016. Mechanotransduction and Metabolism in Cardiomyocyte Microdomains. *Biomed Res Int,* 2016(4081638).

Peters, C., Miller, D. & Giovannucci, D., 2006. Identification, localization and interaction of SNARE proteins in atrial cardiac myocytes. *J Mol Cell Cardiol,* 40(3), pp. 361-74.

Peters, C., Miller, D. & Giovannucci, D., 2006. Identification, localization and interaction of SNARE proteins in atrial cardiac myocytes. *J Mol Cell Cardil,* 3(40), pp. 361-74.

Picard, D., 1993. Steroid-binding domains for regulating the functions of heterologous proteins in cis. *Trends Cell Biol,* 3(8), pp. 278-80.

Ramakrishnan, N., Drescher, M. & Drescher, D., 2012. The SNARE complex in neuronal and sensory cells. *Molecular and cellular neurosciences,* 50(1), pp. 58-69.

Rehmani, T. et al., 2016. *The cardiac specific isoform of tail anchored membrane protein SLMAP1 enhances GLUT4 levels by directing endosomal size and recycling.* Sherbrooke, s.n.

Rindt, H. et al., 1993. In vivo analysis of the murine beta-myosin heavy chain gene promoter. *J Biol Chem,* 268(7), pp. 5332-8.

Rudnicki, M., Braun, T., Hinuma, S. & Jaenisch, R., 1992. Inactivation of MyoD in mice leads to up-regulation of the myogenic HLH gene Myf-5 and results in apparently normal muscle development. *Cell,* 71(3), pp. 383-390.

Sander, J. & Joung, J., 2014. CRISPR-Cas systems for editing, regulating and targeting genomes. *Nat Biotechnol,* 32(4), pp. 347-55.

Santana, L., Cheng, E. & Lederer, W., 2010. How does the shape of the cardiac action potential control calcium signaling and contraction in the heart?. *J Mol Cell Cardiol,* 49(6), pp. 901-903.

Sauer, B. & Henderson, N., 1988. Site-specific DNA recombination in mammalian cells by the Cre recombinase of bacteriophage P1. *Proceedings of the National Academy of Sciences of the United States of America,* 85(14), pp. 5166-5170.

Scherrer, L. et al., 1993. Evidence that the hormone binding domain of steroid receptors confers hormonal control on chimeric proteins by determining their hormone-regulated binding to heat-shock protein 90.. *Biochemistry,* 32(20), pp. 5381-6.

Segev, N., 2001. Ypt/rab gtpases: regulators of protein trafficking. *Sci STKE,* 2001(100).

Seidman, C. & Seidman, J., 1998. Molecular genetic studies of familial hypertrophic cardiomyopathy. *Basic Res.Cardiol,* Volume 93, pp. 13-6.

Severs, N. J., 2000. The cardiac muscle cell. *Bioessays,* 2(22), p. 188–199.

Skach, W., 2000. Defects in processing and trafficking of the cystic fibrosis transmembrane conductance regulator. *Kidney Int,* 57(3), pp. 825-31.

Sohal, D. S. et al., 2001. Temporally regulated and tissue-specific gene manipulations in the adult and embryonic heart using a tamoxifen-inducible Cre protein. *Circ Res.,* 89(1), pp. 20-5.

Söllner, T. et al., 1993. SNAP receptors implicated in vesicle targeting and fusion. *Nature,* 362(6418), pp. 318-24.

Standring, S. & Borley, N., 2008. *Gray's Anatomy: anatomical basis of clinical practice.* London: Churchill .

Statistics Canada, 2014. *Leading causes of death, total population, by age group and sex, Canada, annual,* Canada: CANSIM (database).

Sueishi, M., Takagi, M. & Yoneda, Y., 2000. The forkhead-associated domain of Ki-67 antigen interacts with the novel kinesin-like protein Hklp2. *J Biol Chem,* 275(37), pp. 28888-92.

TA, A. & Van De Ven, W., 1996 . Regulation of gene expression by alternative promoters. *FASEB J,* 4(10), pp. 453-60.

Tora, L. et al., 1989. The human estrogen receptor has two independent nonacidic transcriptional activation functions.. *Cell,* 59(3), pp. 477-87.

Tskhovrebova, L. & Trinick, J., 2003. Titin: properties and family relationships. *Nat Rev Mol Cell Biol*, 4(9), pp. 679-89.

Ullrich, S. et al., 2005. Serum- and glucocorticoid-inducible kinase 1 (SGK1) mediates glucocorticoid-induced inhibition of insulin secretion. *Diabetes*, 54(4), pp. 1090-9.

Verrou, C. et al., 1999. Comparison of the tamoxifen regulated chimeric Cre recombinases MerCreMer and CreMer. *Biol Chem*, 380(12), pp. 1435-8.

Westendorp, B. et al., 2012. The E2F6 repressor activates gene expression in myocardium resulting in dilated cardiomyopathy. *FASEB Journal*, 26(6), pp. 2569-2579.

Wexler, R., Elton, T., Pleister, A. & Feldman, D., 2009. Cardiomyopathy: An Overview. *American family physician*, 79(9), pp. 778-784.

Wielowieyski, P. A. et al., 2000. Alternative splicing, expression, and genomic structure of the 3' region of the gene encoding the sarcolemmal-associated proteins (SLAPs) defines a novel class of coiled-coil tail-anchored membrane proteins.. *J Biol Chem*, 275(49), pp. 38474-81.

Wielowieyski, P. A. et al., 2000. Alternative splicing, expression, and genomic structure of the 3' region of the gene encoding the sarcolemmal-associated proteins (SLAPs) defines a novel class of coiled-coil tail-anchored membrane proteins.. *J Biol Chem*, 275(49), pp. 38474-81.

Wigle, J. et al., 1997. Molecular cloning, expression, and chromosomal assignment of sarcolemmal-associated proteins. A family of acidic amphipathic alpha-helical proteins associated with the membrane. *J Biol Chem*, 272(51), pp. 32384-94.

Woodcock, E. & Matkovich, S., 2005. Cardiomyocytes structure, function and associated pathologies. *The International Journal of Biochemistry & Cell Biology*, 37(9), pp. 1746-51.

Wu, S., Ying, G., Wu, Q. & Capecchi, M., 2007. Toward simpler and faster genome-wide mutagenesis in mice. *Nat Genet*, 39(7), pp. 922-30.

Xiao, S. & Shaw, R., 2015. Cardiomyocyte protein trafficking: Relevance to heart disease and opportunities for therapeutic intervention. *Trends Cardiovasc Med*, 25(5), pp. 379-89.

Xie, C. et al., 2016. Genome editing with CRISPR/Cas9 in postnatal mice corrects PRKAG2 cardiac syndrome. *Cell Res*, 26(10), pp. 1099-1111.

Yacoub, M., 2014. Decade in review--cardiomyopathies: Cardiomyopathy on the move. *Nat Rev Cardiol*, 11(11), pp. 628-9.

Yang, X. et al., 1999. Echocardiographic assessment of cardiac function in conscious and anesthetized mice. *Am J Physiol*, 277(5), pp. 1967-74.

Yin, Z., Ren, J. & Guo, W., 2015. Sarcomeric Protein Isoform Transitions in Cardiac Muscle: A Journey to Heart Failure. *Biochimica et biophysica acta,* 1852(1), pp. 47-52.

Yudowski, G., Puthenveedu, M., Henry, A. & von Zastrow, M., 2009. Cargo-mediated regulation of a rapid Rab4-dependent recycling pathway. *Mol Biol Cell,* 20(11), pp. 2774-84.

Zhang, Y. et al., 1996. Inducible site-directed recombination in mouse embryonic stem cells. *Nucleic Acids Res,* 24(4), pp. 543-8.

Zhao, J. et al., 2016. Cardiac Gab1 deletion leads to dilated cardiomyopathy associated with mitochondrial damage and cardiomyocyte apoptosis. *Cell Death Differ,* 23(4), pp. 695-706.

Zhu, G. et al., 2004. Structural basis of Rab5-Rabaptin5 interaction in endocytosis. *Nat Struct Mol Biol,* 11(10), pp. 975-83.

Chapter 6: Appendices

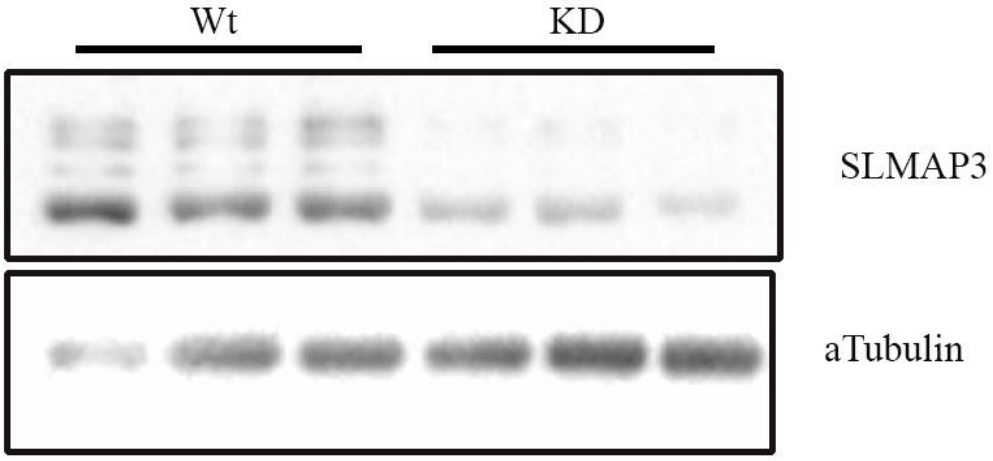

Appendix 1. Presence of *SLMAP3 variants in KD animals.* The expression levels of SLMAP3 variants of ~91 KDa compared with 83kDa are difficult to quantify in KD animals due to their low abundance. Copyright (2017) of Balwant Tuana laboratory at the University of Ottawa.